

Cite this: *Mater. Adv.*, 2022,  
3, 2268Received 17th October 2021,  
Accepted 16th December 2021

DOI: 10.1039/d1ma00961c

rsc.li/materials-advances

## Recent advances in the targeted delivery of paclitaxel nanomedicine for cancer therapy

Faisal Raza,<sup>a</sup> Hajra Zafar,<sup>†\*a</sup> Muhammad Wasim Khan,<sup>b</sup> Aftab Ullah,<sup>c</sup>  
Asif Ullah Khan,<sup>d</sup> Abdul Baseer,<sup>e</sup> Rameesha Fareed<sup>f</sup> and Muhammad Sohail<sup>g</sup>

Cancer cases have reached an all-time high in the current era. Thus, there is a need to develop advanced therapeutic methods that can effectively inhibit the proliferation of precancer and malignant tumors. These strategies should exhibit potential to manage cancer and improve the effectiveness of conventional therapeutic agents. Regarding cancer, paclitaxel is one of the most effective chemotherapeutic drugs. Thus, nanomedicine of paclitaxel has extended its use in the efficient management of cancer. In this review, initially, the use of the promising compound paclitaxel is highlighted for chemotherapy. Subsequently, the state of the art of nanoformulations of paclitaxel for its use against cancer are discussed. The properties and applications of paclitaxel nanomedicine are highlighted and several types of paclitaxel nanomedicine systems are discussed. Finally, the current challenges and future perspectives are reviewed.

### 1. Introduction

Cancer is considered one of the most serious health-related threats worldwide. Despite the rapid development of new therapeutic approaches, malignant tumors are still one of the leading causes of human death globally.<sup>1,2</sup> In the past few decades, the conventional approach to treating cancer has included chemotherapeutic agents, surgical removal and radiation. However, radiation and chemotherapy reduce the quality of life due to their serious side effects and toxicity. They also run the risk of inducing resistance in cancer cells, rendering them unaffected by chemotherapy and radiotherapy.<sup>3</sup> Thus, these obstacles and challenges have made achieving the desired patient outcomes difficult; hence, scientists are currently searching for novel alternative treatments.<sup>4</sup> Recently, the anticancer properties of many natural compounds have been discovered, resulting in their use in the treatment and prevention of cancer as alternatives to the conventional agents. Examples of these entities with less side effects include paclitaxel (PTX), lycopene, curcumin, folate,

gingerol, and resveratrol.<sup>5–7</sup> Recently, PTX has become very popular due to its extensive anticancer activity.<sup>8–10</sup> Paclitaxel was first isolated from Pacific yew or *Taxus brevifolia* bark. Its physical properties include a white powder crystalline in nature and it has a melting point of about 210 °C. As one of the most effective anticancer drugs, paclitaxel is employed in treating lung, breast, and ovarian cancer.<sup>11,12</sup> It works by stabilizing the microtubules of cells and inhibiting the late G2 or M phases of the cell cycle, causing cells to die. However, to increase its limited clinical use owing to its poor water solubility of around 0.4 µg mL<sup>-1</sup>, paclitaxel is formulated in combination with Cremophor EL with the brand name “Taxol”. Cremophor EL consists of castor oil and dehydrated ethanol. However, this solvent system is associated with serious side effects such as allergic reactions and a change in the pharmacokinetic profile of PTX.<sup>13</sup> Thus, to prevent the hypersensitivity reaction, the drug is infused over a longer period together with the use of steroids and antihistamines. As mentioned earlier, the solvent Cremophor EL also alters the drug kinetics, leading to non-linearity.<sup>14</sup> Drug resistance is also a common phenomenon observed with the use of PTX because it is a substrate of an efflux pump called P-gp, which decreases the intracellular concentration of the drug. Thus to combat this, drugs that exhibit p-gp inhibitory action were concurrently administered, such as Verapamil<sup>15</sup> and PSC 833,<sup>16</sup> but this led to toxicity and changed the pharmacokinetics and tissue distribution of paclitaxel.<sup>17,18</sup>

Nano drug delivery systems enhance the solubility of paclitaxel and other hydrophobic drugs and are less toxic. A PX albumin-bound NP formulation, Abraxane<sup>®</sup>, was first FDA approved for treating metastatic breast cancer in 2005. It has a particle size of about 130 nm<sup>19</sup> and was shown to be less toxic

<sup>a</sup> School of Pharmacy, Shanghai Jiao Tong University, Shanghai 200240, P. R. China. E-mail: faisalraza@sjtu.edu.cn, hajrazafar@sjtu.edu.cn

<sup>b</sup> School of Pharmaceutical, Shandong University, P. R. China

<sup>c</sup> Department of Pharmacy, Shantou University Medical College, Shantou, 515041, P. R. China

<sup>d</sup> Hangzhou Grand Biologic Pharmaceutical Inc, P. R. China

<sup>e</sup> Department of Pharmacy, Abasyn University, Peshawar, Pakistan

<sup>f</sup> Riphah Institute of Pharmaceutical Sciences, Riphah International University Islamabad, Pakistan

<sup>g</sup> School of Pharmacy, Yantai University, Shandong, 264005, China

<sup>†</sup> These authors contributed equally to this work.



than PTX.<sup>20–23</sup> Also, this nanoformulation did not require a long infusion time and only needed to be infused for 30 min without premedication. However, whether Abraxane<sup>®</sup> improves the prognosis or fixes the efflux pump-mediated drug resistance has not been established.<sup>24</sup> This means that there is still a need to develop new PTX formulations. Nanomedicine systems such as polymeric, cyclodextrin and inorganic NPs, carbon nanotubes and polymer conjugates are discussed in this review, focusing on treating cancer.

## 2. Essential properties of paclitaxel nanomedicine

### 2.1 Particle size

The ideal nanomedicine diameter is in the range of 10–100 nm for cancer treatment.<sup>25,26</sup> The particle size of nanomedicine cannot be too small otherwise, it will undergo rapid renal elimination; hence, the sieving coefficient of the glomerular wall determines where the particle size range starts.<sup>27</sup> The pore size for tumors is in the range of 380–780 nm, but normally particles less than 2 nm are permeable through the vessels.<sup>28,29</sup> It has been reported that particles sized in the submicron range can leak out of the circulation and concentrate in tumors, improving the drug penetration and retention (EPR) effect. However, some studies showed that particles with a size in the range of 100–150 nm with a positive charge enter tumor cells more easily.<sup>30–32</sup> Fig. 1 shows the properties of nanoparticle drug delivery systems that determine their activity.

### 2.2 The appropriate surface properties

The high contact surface area of nanoparticles yields more interactions between tumor cells and drug particles.<sup>33,34</sup> To be internalized by tumor cells, nanoparticles need to have a size in

the range of 50 to 100 nm, have slight surface charges, either positive or negative, and have negligible interactions.<sup>32,35</sup> Nanoparticles that are cationic lead to better interactions between the cells and nanoparticles and improved uptake of drug nanoparticles because the cell membrane is negatively charged, as shown in Fig. 1 and 2.<sup>35</sup>

### 2.3 The ligands that target nanomedicine

The interactions between nanoparticles and cells are also defined by the ligands on the surface of nanoparticles.<sup>36</sup> For instance, targeting the receptor proteins present on the tumor cell membrane for optimized binding with nanoparticles is enhanced by associating them with proteins, antibodies, or other proteins.<sup>35</sup> Lower doses of drugs are required to achieve a therapeutic effect when more of the drug gets concentrated in the cells, which is the case with nanoparticles as well. This internalization and uptake of nanodrug molecules depend on their surface properties and particle size.<sup>37</sup> It is believed that nanoformulations can also circumvent the problem of drug resistance, which is mediated by surface protein pumps, because nanoparticles are endocytosed into the cell and this process not dependent on surface mechanisms.<sup>35,38</sup>

### 2.4 Pharmacokinetic properties

In terms of pharmacokinetics, paclitaxel has a high molecular weight of 853.0 g mol<sup>-1</sup> and poor water solubility. CYP2C8 metabolizes it into its major metabolite 6 $\alpha$ -hydroxypaclitaxel and CYP3A4 into two minor metabolites. It undergoes biliary excretion with an elimination half-life of 5.8 h when infused for 6–24 h.<sup>39</sup> It does not penetrate the blood–brain barrier but is distributed in ascitic fluid.<sup>40</sup> During its continuous infusion, the plasma concentrations rise and drop immediately upon cessation of the infusion. It is also a substrate of some enzyme systems including ABC efflux pumps consisting of p-gp and BCRP.<sup>41,42</sup> Paclitaxel is not orally bioavailable due to the efflux action of these ABC pumps, which transport the drug retrogradely into the intestinal lumen.<sup>43</sup> The hepatic influx or uptake of paclitaxel is mediated by organic anion transporter (OAT) type 1B3 and OAT 2 for renal influx.<sup>44</sup> Any genetic differences in these transporters account for the variable pharmacokinetics of paclitaxel. The phenomenon of autoinduction is also thought to be minimally involved when paclitaxel upregulates CYP3A4 by activating the pregnane X receptor.<sup>45</sup> A newer approach to study the pharmacokinetics of paclitaxel is the use of the AUC of the unbound drug to elucidate the neutropenia associated with both 1 h and 3 h infusions using empirically-designed threshold models. Another well-supported hypothesis is that the solvent used in paclitaxel formulations, Cremophor EL, is distributed according to the total blood volume linked with the patient's BSA.<sup>45,46</sup> Therefore, it is strongly believed that the variable pharmacokinetics of paclitaxel are due to the differences in BSA, which can lead to the shortening of the infusion time from 3 h to 1 h.<sup>47</sup> The usually studied dose range of paclitaxel is 15–825 mg with an infusion time of 0.5–96 h. A dose of 175 mg of the paclitaxel formulation with Cremophor, when infused over 3 h led to a median maximum concentration of 5.1  $\mu\text{mol L}^{-1}$ . This particular formulation using Cremophor follows non-linear kinetics when infused for short periods



Faisal Raza

*Faisal Raza is currently a PhD student at the School of Pharmacy, Shanghai Jiao Tong University (SJTU), China. He has broad research interests in the areas of pharmaceuticals and drug delivery. His specific field of research focuses on the design and synthesis of novel peptides and polymers for drug delivery, analysis of therapeutic efficacy and toxicity studies in cancer mouse models, formulating and developing advanced drug delivery*

*systems for poor water soluble anticancer drugs, developing stimulatory responsive nanomedicine and biomimetic nanotechnology for cancer therapy. He has authored/co-authored 30+ research and review papers in well-reputed SCI journals, including Biomaterials, Advanced Healthcare Materials, Journal of Materials Chemistry B and Biomaterials Science with a total impact factor of 150+.*



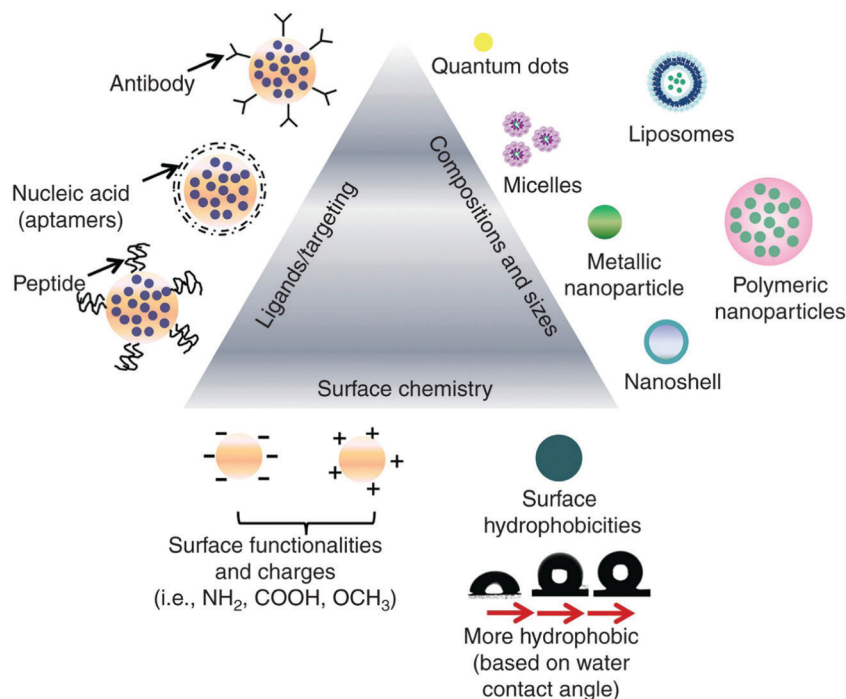


Fig. 1 Various examples of the external factors that impact the interactions between drugs and cells. This information can be utilized when designing nanomedicine targeting a specific function. Reproduced with permission.<sup>32</sup> Copyright 2014, Taylor & Francis Online.

(<6 h).<sup>48</sup> For understanding the toxicity and effectiveness profile of PTX, the time above the threshold drug concentration in plasma is used, which is  $0.05 \mu\text{mol L}^{-1}$  for paclitaxel.<sup>49</sup> How effectively the tumor responds to paclitaxel depends on the type of cancer and the other chemotherapeutics used in combination and the order of their administration.<sup>50</sup>

### 2.5 Biostability

Generally, small molecules are not therapeutically ideal as anticancer agents due to their poor water solubility, selectivity, and drug resistance; hence, many techniques have been employed to reduce these obstacles. One of these methods is the use of nanoparticles, which significantly improve their solubility and subsequent bioavailability.<sup>51,52</sup> The use of a polymeric conjugate prolongs the duration of action and results in the better permeation and retention of the anticancer agent.<sup>51</sup> In terms of physicochemical properties, paclitaxel is nonselective for tumors and insoluble in water, and thus insufficiently bioavailable in aqueous solution. As mentioned previously, paclitaxel is formulated using Cremophor EL and ethanol to treat several cancers and also been homogenized into an emulsion for better water solubility. The most advanced polymeric paclitaxel conjugate is the one with poly(L-glutamic acid) and designated as CT-2103, which is under investigation in clinical trials. To improve the paclitaxel-carrying capacity, the poly(L- $\gamma$ -glutamylglutamine) consists of double carboxylic groups on polyglutamic acid, the parent chain.<sup>53</sup> The resulting paclitaxel-poly(L- $\gamma$ -glutamylglutamine) should have a macromolecular weight of around 80 kDa for enhanced penetration and collection of the drug in the tumor. Conjugating paclitaxel with a polymer backbone also affects its urinary and fecal

excretion.<sup>54,55</sup> The physicochemical properties of paclitaxel can also be modified using an epoxidized copolymer, which forms nanoparticles with a lower micelle size and critical micelle concentration and better loading capacity and encapsulation.<sup>56,57</sup> Paclitaxel is a hydrophobic drug, and hence shows more efficient release from epoxidized nanomicelles, which are also biodegradable.<sup>58,59</sup> The pharmaceutical excipients studied as potential conjugates for paclitaxel are cyclodextrins. Recently, it was discovered that cyclodextrin is endocytosed by cells. A study was carried out to check the efficacy of using various cyclodextrins to facilitate the cellular uptake of fluorescent paclitaxel.<sup>60,61</sup> However, results showed the concentration of paclitaxel in the intestinal cells with limited permeability through the cells.<sup>62</sup> The methodology of conjugating paclitaxel with a water-soluble polymeric carrier holds great potential in terms of improving its physicochemical and pharmacokinetic properties.<sup>63</sup>

## 3. Advantages of paclitaxel nanomedicine in the delivery of drugs

Nanomedicine has become very popular recently and employed to treat cancers.<sup>64</sup> PTX is an effective chemotherapy drug and has been a part of numerous nanoformulations, which have several advantages over conventional therapy.<sup>65</sup> Firstly, the water solubility of PTX can be greatly improved when it is conjugated with hydrophilic polymers or when encapsulated in liposomes. Secondly, due to their smaller particle size, the delivery of PTX is targeted to the tumor due to the increased permeability and retention effect (EPR).<sup>66,67</sup> Thirdly, these



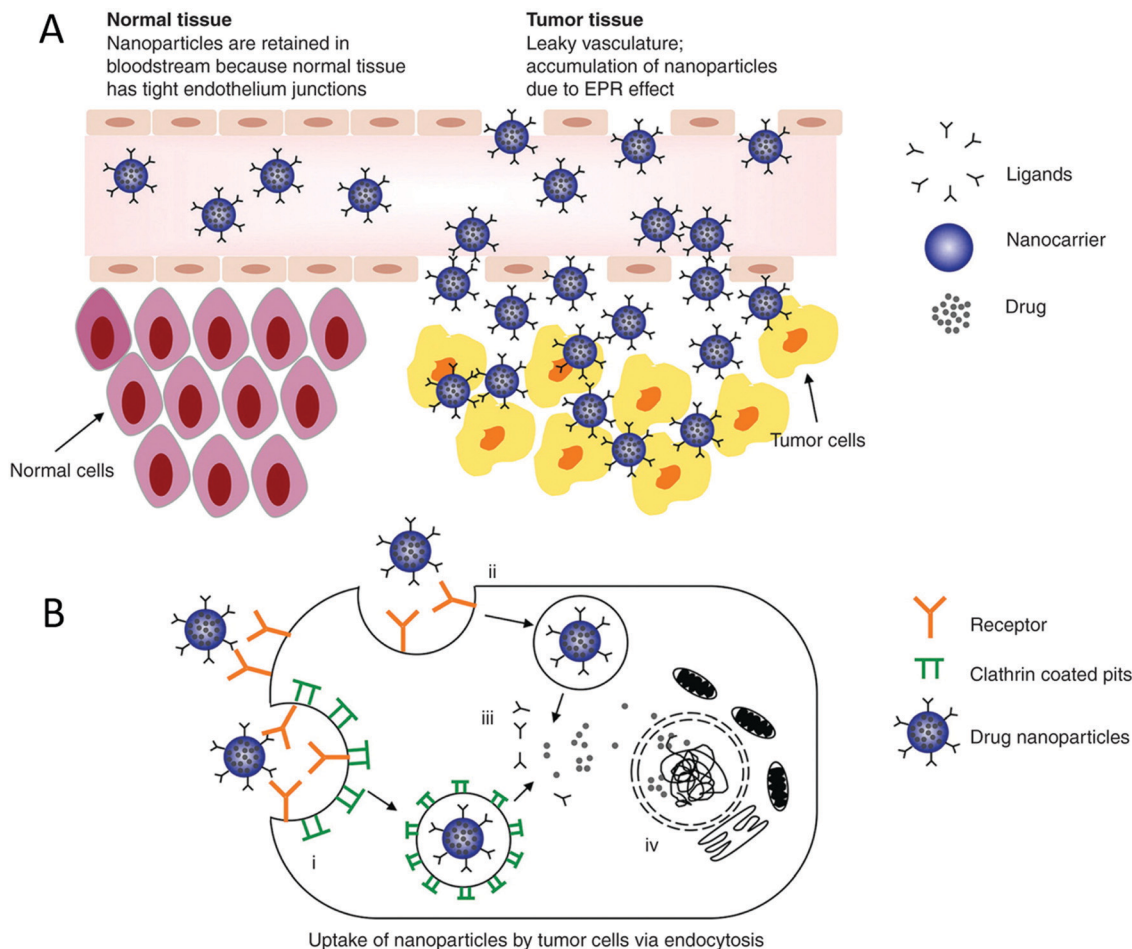


**Fig. 2** (A) Goal of nanoparticles is to make use of increased vessel permeability and retention effect to extravasate, concentrate in cancerous tissue and endocytose into the cell, where they release the drug. On the contrary, the nanoparticles would stay in the blood and not cross the cell membrane due to the tight junctions present in the tissues. (B) Internalization of small particles occurs via the following mechanisms: clathrin-mediated and independent endocytosis. This mechanism is used when increasing the uptake of the drug into the cells, and eventually the nucleus depending on the particle size. Reproduced with permission.<sup>32</sup> Copyright 2014, Taylor & Francis Online.

nanoparticles are not caught by the surveillance of the reticuloendothelial system (RES) present in normal tissues, and thus reduce the drug-associated side effects.<sup>68</sup> This also sets the MTD or maximum tolerated doses of the nanoformulation to a higher number.<sup>69</sup> It is important to note that to circumvent the RES surveillance, the surface of nanoparticles should contain polyethylene glycol (PEG).<sup>70</sup> This also improves the pharmacokinetic profile of PTX, which increases its half-life and its subsequent tissue accumulation.<sup>71</sup> As previously mentioned, the surface of nanoparticles can be made to contain ligands that aid the targeted delivery of drugs and increase the uptake of drugs by the cells, thereby reducing their side effects.<sup>72,73</sup>

## 4. Recent applications of PTX nanomedicine for the treatment of cancer

Lately, numerous PTX nanoformulations have been designed to improve the delivery of PTX to the tumor cells. They are used to

improve the water solubility and stability of PTX. The ideal nanoformulation has better activity compared to conventional or free PTX, while also sparing normal cells. Fig. 3 shows the different types of PTX nanomedicines utilized for the treatment of cancer and Table 2 includes a summary of the literature findings.

### 4.1 Tumor microenvironment-responsive micelles for the delivery of paclitaxel

**4.1.1 pH-Responsive micelles.** Because of its convenience and excellent association with tumor tissues, pH as an internal stimulus has received much interest.<sup>74</sup> There are two major ways to make pH-sensitive polymeric micelles that are resilient in the bloodstream and quickly depolymerize once they reach the tumor site. One depends on micellar materials being hydrolyzed, while the other relies on the protonation and deprotonation of proton donor moieties. The acidic microenvironment of the extracellular matrix of tumors, endosomes, and lysosomes vary.<sup>75</sup> The drug will be delivered outside or in cancer cells based on the susceptibility of the micelle to pH,



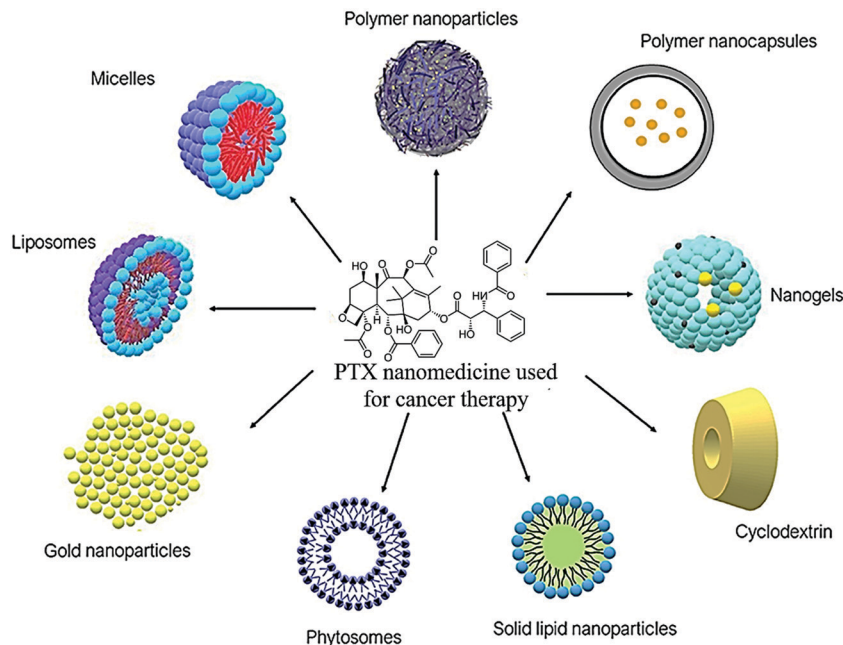


Fig. 3 Different PTX nanomedicines used in cancer treatment in the literature.

producing various anti-tumor actions. Clinically, it has been observed that the side effects of anticancer agents on the healthy organs of patients and the drug resistance exhibited by tumor cells are the main reasons why chemotherapy is not as effective as it should be.<sup>76,77</sup> Thus, to achieve targeted drug delivery to tumors, it is important for chemotherapeutic agents to be freed from their carriers and efficiently escape from lysosomes or endosomes.<sup>78,79</sup> Gao *et al.* designed and formulated YPSMA-1-modified pH-sensitive polymeric micelles, which could selectively bind to PSMA and ensure the targeted delivery of paclitaxel to the cancer cells *via* the pH-sensitive diblock copolymer poly(2-ethyl-2-oxazoline)-poly(D,L-lactide) (PEOZ-PLA) and YPSMA-1-PEOZ-PLA. <sup>1</sup>H NMR and gel permeation chromatography were used to formulate and characterize HOOC-PEOZ-PLA, consisting of a CMC (critical micelle concentration) of 5 mg L<sup>-1</sup>. YPSMA-1-modified micelles were synthesized with a diameter of 30 nm, which rapidly released the drug at the endo/lysosomal pH. Confocal microscopy was used to visualize this rapid escape ability from lysosomes or endosomes. The escape of the pH-sensitive micelles from the lysosome and endosome was also traced in real-time using confocal microscopy. The cytotoxicity profile of paclitaxel was improved using the YPSMA-1-modified micelles, which enhanced the influx of the drug in PSMA-positive 22Rv1 cells. This finding was corroborated using flow cytometry and confocal microscopy. Compared with the unmodified micelles and Taxol<sup>®</sup>, the YPSMA-1-modified micelles in 22Rv1 xenograft-bearing nude mice exhibited improved anticancer effect with minimal systemic toxicity owing to the selectivity and pH-sensitivity of these micelles. These findings suggest that pH-sensitivity, together with YPSMA-1 modification, is a promising approach to deliver chemotherapeutics in PSMA-positive cancers, as shown in Fig. 4.<sup>80</sup>

Similarly, Gao *et al.* synthesized cyclic RGDyK (cRGDyK)-conjugated pH-sensitive polymeric micelles with the pH-sensitive

copolymer poly(2-ethyl-2-oxazoline)-poly(D,L-lactide) (PEOZ-PLA) and cRGDyK-PEOZ-PLA for the delivery of paclitaxel directly to cancer cells with improved anticancer activity. With a 28 nm diameter, these micelles rapidly released paclitaxel at the endosomal or lysosomal pH, thereby improving the paclitaxel-associated cytotoxicity in PC-3 cells. This was achieved by increasing the cellular influx of the drug with the help of integrin  $\alpha\beta3$  expression in tumor cells. *In vivo* real-time near IR fluorescence imaging corroborated the targeted activity of the micelles in PC-3 tumor-bearing nude mice. The cRGDyK-conjugated micelles had better anticancer activity than the unmodified micelles in combination with Taxol in PC-3 xenograft-bearing nude mice. This is because of the pH sensitivity and targeted activity of the conjugated micelles, which also showed minimal systemic toxicity. This shows that cRGDyK-conjugated pH-sensitive polymeric micelles have potential use in the targeted delivery of chemotherapeutics in cancers densely populated with integrin  $\alpha\beta3$ , as seen in Fig. 5.<sup>81</sup>

To determine whether the proposed nanoformulation will be successful, scientists used a 2D monolayer cell culture model. However, the performance of the model did not correlate 100% with the *in vivo* results of the nanoformulation. Therefore, multicellular tumor spheroids (MCTSs) were used as an intermediate model, which gave a 3-dimensional representation. W. Du *et al.* compared and contrasted the results of both the conventional monolayer cell cultures and the 3D MCTS. This research group also analyzed the cytotoxicity of free and conjugated paclitaxel, which was associated with poly(ethylene glycol methyl ether acrylate)-*b*-poly(carboxyethyl acrylate) or (POEGMEA-*b*-PCEA-PTX) block copolymer. A diamino nondegradable crosslinker was used in the core of the micelles and its impact of their stability was investigated. According to the tumor cell culture, all the micellar variants (IC<sub>50</sub>: 193–271 nM)



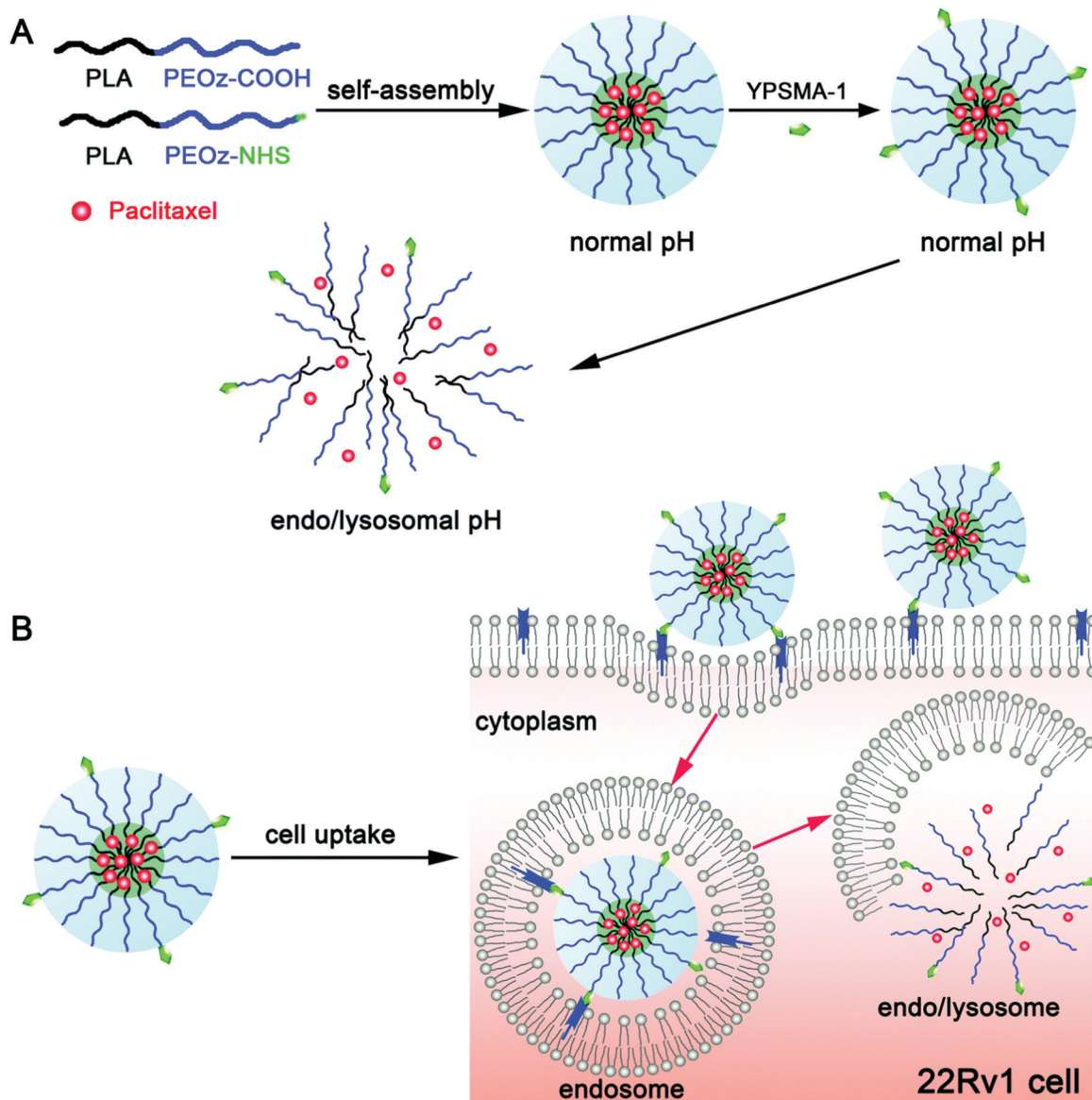


Fig. 4 (A) Acid-triggered drug release from pH-sensitive micelles is schematically illustrated together with multifunctional polymeric micelles, which were modified using YPSMA-1. (B) Cellular influx together with intracellular trapping of YPSMA-1-modified PEOz-PLA polymeric micelles is illustrated in cancer cells. Reproduced with permission.<sup>80</sup> Copyright 2015, The Royal Society of Chemistry.

were shown to have less toxicity than the free drug ( $IC_{50}$ : 15.2 nM). However, the results of the 3-dimensional MCTs revealed that the micelles exhibited a greater toxicity profile than free PTX. Thus, DAO-cross-linked POEGMEA-*b*-PCEA-PTX conjugate micelles have potential use as a carrier in nanoformulations used in cancer treatment owing to their improved anti-tumor activity when cross-linked with MCTS, which according to Fig. 6, can be used to integrate 3D structures in *in vitro* tests.<sup>82</sup>

Preferred anti-tumor nanoformulations include a controlled release rate and drug distribution that is selective for the tumor. An anisamide-conjugated *N*-octyl-*N,O*-maleoyl-*O*-phosphoryl chitosan (a-OMPC) formed amphiphilic micelles whose release rate was pH dependent and highly bonded with Sigma-1 receptor, which had an increased expression in tumors, was formulated by Qu *et al.* to deliver paclitaxel to tumor cells.

The pH-dependent drug release depends on the maleoyl and phosphoryl groups, which become hydrophobic at the acidic lysosomal/endosomal pH. It was shown that improved internalization occurred due to the attraction of anisamide to the Sigma-1 receptor in the paclitaxel-loaded a-OMPC micelles (PTX-aM). The resulting efficient release of paclitaxel in the endosomes/lysosomes increased the cytotoxicity in cancer cells. It was also shown that even after 24 h of administration, PTX-aM concentrated in large amounts at the cancer site, which led to anticancer activity and better survival in PC-3 tumor xenograft-bearing mice. This chitosan derivative can be used for the targeted delivery of cancer drugs because OMPC did not cause any hemolysis or acute toxicity, as shown in Fig. 7.<sup>83</sup>

**4.1.2 Redox-responsive polymeric micelles.** GSH, like pH, is another stimulus that has attracted considerable interest.



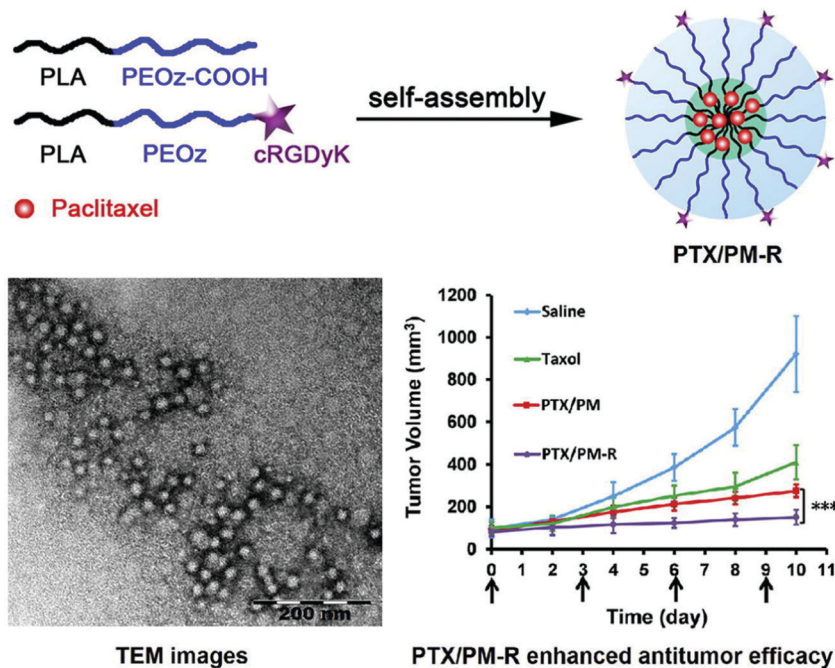


Fig. 5 Scheme of how targeted PTX delivery for improved anticancer activity can be achieved by cRGDyK conjugated pH-sensitive polymeric micelles. Reproduced with permission.<sup>81</sup> Copyright 2015, Elsevier.

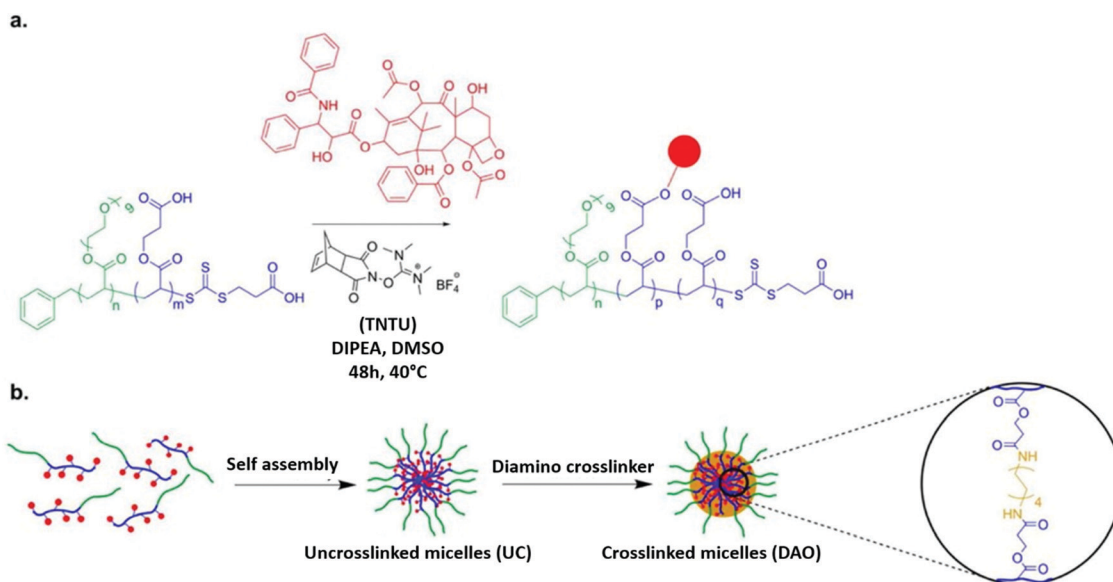


Fig. 6 (a) RAFT polymerization together with solid-phase peptide synthesis (SPPS) reagent is employed to conjugate PTX with block copolymer. (b) Utilizing nondegradable diamine crosslinker, the polymer–paclitaxel conjugate is cross-linked and self-assembled. Reproduced with permission.<sup>82</sup> Copyright 2015, the American Chemical Society.

GSH is present in abundance in cancer tissues. The GSH concentrations in the intracellular compartments are 100–1000 times greater than that in the external compartments, and the GSH concentrations in tumor tissues are 4-fold higher than that of normal cells.<sup>84</sup> Thus, redox ability can be used to discriminate between the internal and external surroundings, as well as normal and malignant cells. The most common way

to make redox-sensitive micelles is to make an amphiphilic polymer with hydrophilic and hydrophobic sections connected by a GSH-responsive linker, then self-assemble the composite material to form a core-shell structure in the aqueous phase.<sup>85</sup> This type of material contains a small number of redox-sensitive bonds, where the most common is the disulfide bond. This method has been used to produce a number of



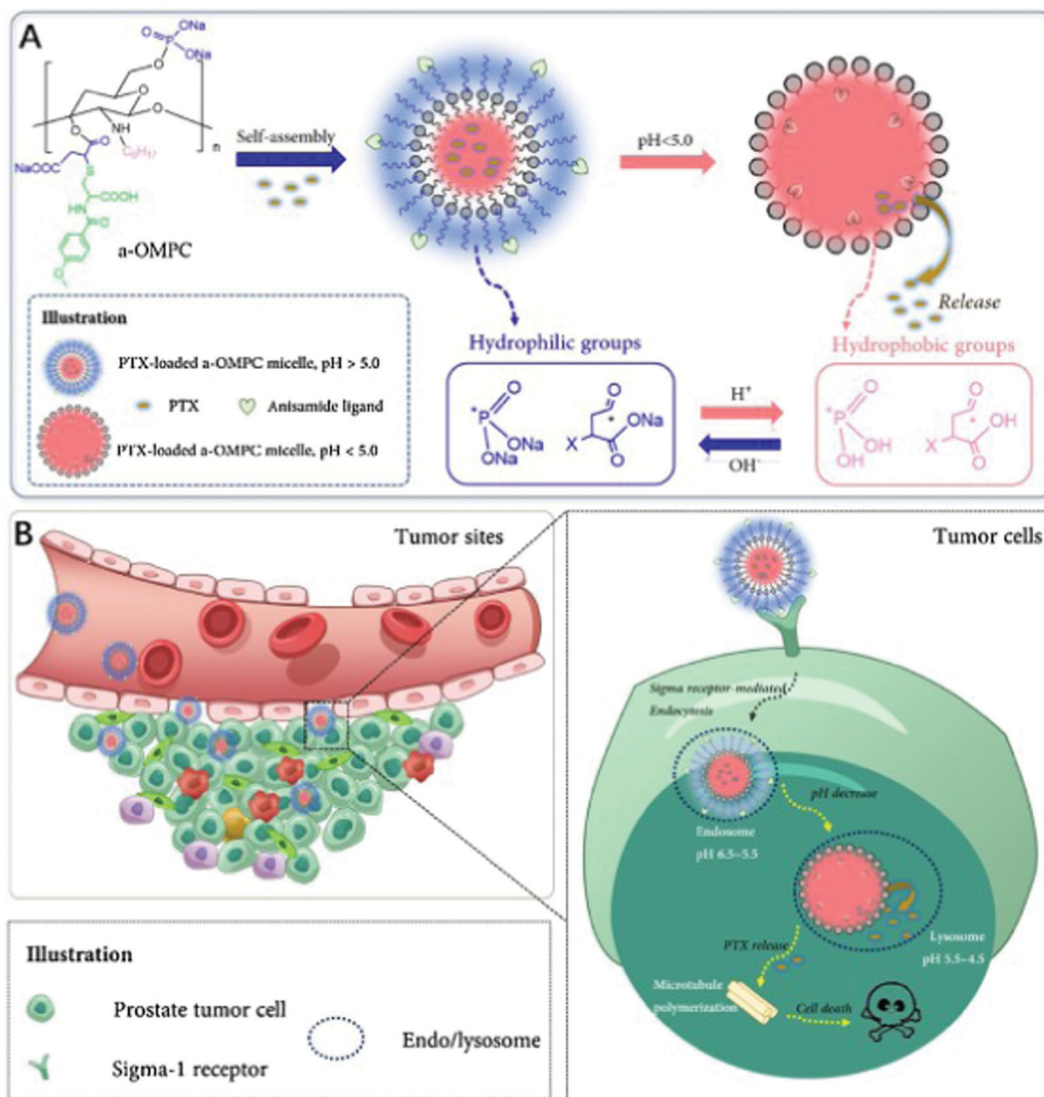


Fig. 7 PTX micelles based on amphiphilic chitosan and their affinity for treating cancer-specific to Sigma-1 receptors. (A) In a neutral medium, a-OMPC changes to hydrophilic PTX-aM loaded with paclitaxel. At acidic pH, it can become hydrophobic due to the protonation of phosphate and maleate stimulated by pH. This results in the release of the drug. (B) Sigma-1 receptor-mediated pathway helps PTX-aM concentrate at the cancer site and cross into the PC-3 cell owing to the improved permeation and retention (EPR) effects. PTX-aM is then captured by the lysosomes or endosomes, after which it becomes hydrophobic at low pH, which destabilizes the micellar structure and results in immediate drug release, thereby improving the anticancer effect. Reproduced with permission.<sup>83</sup> Copyright 2020, Elsevier.

redox-sensitive micelles. Micelles having redox-sensitive regions have good stability in the bloodstream but are destroyed when they reach the tumor site.<sup>85</sup> However, despite the fact that several micelles have been produced as drug carriers, only a tiny percentage has been proven to improve the therapeutic effectiveness owing to their unpredictable *in vivo* activity. The majority of these nanomedicines have poor targeting efficacy and drug release, resulting in poor therapeutic results. The hydrophobic and hydrophilic moieties of HA-SS-tocopherol succinate (TOS) were linked through a disulfide bond to form a conjugate.<sup>85</sup> Through the attachment of HA to CD44 receptors, the PTX-loaded micelles were successfully targeted to tumor locations, and the micelles were subsequently absorbed *via* endocytosis. 60% PTX was released from the micelles in a

phosphate buffer (PBS) solution having 10 mM GSH, which was much higher than the 30% released in the medium without GSH. The micelles were substantially more effective in killing CT26 mouse colon cancer cells that had overexpressed the CD44 receptor. The *in vivo* investigation revealed that when cancer-bearing mice were given PTX-loaded redox-sensitive micelles, they had a 100% survival rate, whereas the survival rates of the saline and Taxol groups were just 60% and 40%, respectively. Tumor cells need more glucose than normal cells, and glucose entry requires specific membrane proteins.<sup>86</sup> In this regard, aminoglucose (AG)-conjugated redox-responsive nanomicelles of PEG were synthesized.<sup>86,87</sup> To achieve targeted distribution to tumor areas, the polymer was modified with glucosamine. The disulfide bond was created to achieve





controlled drug release. In the context of GSH, the rate of PTX release was considerably enhanced. The intracellular release pattern revealed that 40% of the PTX was discharged from the drug-loaded micelles after 48 h in the absence of GSH, 53% in the presence of 5 mM GSH, and 78% in the presence of 10 mM GSH. With an increase in the concentration of GSH, the disulfide bond was broken and the release of PTX occurred more rapidly. The modified micro-micelles substantially decreased the cell survival compared to the unmodified groups. The anticancer effect was shown to be the maximum in *in vivo* testing. Furthermore, compared to Taxol, the micelles did not result in a substantial drop in body weight.<sup>84,87</sup>

**4.1.3 Enzyme-responsive polymeric micelles.** Because of their high selectivity and outstanding catalytic characteristics, enzymes play a crucial role in numerous biological processes throughout the body.<sup>88</sup> Enzymes are intimately linked to human health, where aberrant enzyme expression is associated with numerous disorders. Many malignancies have the aberrant production of enzymes such as proteases, peptidases, and lipases,<sup>89</sup> and thus these enzymes can be used as an internal stimulation to enhance the drug release at the tumor site. Enzyme-responsive polymeric micelles are more desirable than pH or redox-responsive micelles due to their selectivity and efficiency, given that peptide substrates have superior biocompatibility and biodegradability. MMPs, or endopeptidases, can destroy the ECM proteins that are overexpressed in the extracellular niches of tumors, which play a key role in tumor growth and metastasis.<sup>90</sup> MMP-2 and MMP-9 are two of the most investigated MMPs.<sup>91</sup> In one work, the MMP-sensitive peptide GPLGVRGDG was included in a block copolymer.<sup>92</sup> Genexol-PM was used as it was proven to have higher effectiveness and lower toxicity than free PTX. The micelles had a long circulation time and considerable accumulation in tumor tissues, although the anti-tumor activity of PTX was hampered by its intracellular internalization. The peptide was susceptible to MMP2 up-regulation at the tumor site, and MMP2 degraded it at a particular site.<sup>88</sup> Because the shape of the micelles did not change considerably in the presence of MMP-2, the PTX release rate did not differ significantly from that in the absence of MMP-2. The hydrophilic portion was cleaved and the residual peptide sequence interacted with tumor cells to improve cellular internalization.<sup>93</sup> The tumor volume increased only 1.9-fold in the case of the new micelles. The micelles carrying an enzyme-sensitive peptide exhibited superior anticancer activity, according to the findings. The PEG2000-MMP2-sensitive peptide was produced in another work to encapsulate PTX.<sup>93</sup> The exterior shell of the micelle was composed of PEG2000, which acts as a protective chain. The tumor-targeting intermediate layer was produced by the MMP2 sensitive peptide, which served as a linker. TAT peptide and PEG-PE were used to make the cell permeating middle layer and inner core of the micelle, respectively. Under the activation of MMP2 in the ECM, the coupling of the MMP2-responsive peptide was broken, and the protective PEG shell was eliminated. The MMP2-sensitive micelles improved tumor penetration and cell absorption of the micellar load in the *in vivo* tumor retention experiment.<sup>90,93</sup>

## 4.2 Biomimetic nanomedicine for paclitaxel delivery

Cells, as the key element of life, have evolved to interact efficiently with their surroundings. Cells are usually specialized for a certain function, and consequently they have distinct biological components that allow them to perform their activities. Red blood cells (RBCs), for example, are important for delivering oxygen and may travel for long periods of time.<sup>94</sup> Platelets have developed to be able to circulate for extended periods in the bloodstream, with targeted features that enable them to reach disease locations and aid wound repair.<sup>95</sup> Cancer cells usually display immune evasion qualities that aid in their survival, despite the fact that they are harmful to human health.<sup>96</sup> Eventually, the biointerfacing capacities of various cell types are mostly dictated by their outer membrane layer, which has specific protein, lipid, and carbohydrate patterns. A novel type of biomimetic nanovehicle with cell-mimicking capabilities, cell membrane cloaked nanoparticles, were produced by directly transferring the cell membrane to the surface of a nanoparticles.<sup>97</sup> The feasibility of the cellular membrane coating technique was initially proven utilizing the RBC membrane in a proof-of-concept study.<sup>98</sup> To aid in their extended transit for up to four months, RBCs release a multitude of surface markers, including the “don’t eat me” signal CD47 and a plethora of complement regulating proteins.<sup>99</sup> Membranes were produced from RBCs through hypotonic processing, and then coextruded with polymer cores to make RBC membrane-coated nanoparticles. The resultant nanoparticle formulations had a longer circulation duration and an elimination half-life of around 40 h in an *in vivo* mouse model compared to the control. The long circulation feature native was attributed to the RBC membrane, highlighting the possibility of nanoparticle surface modification with cell membranes. The treatment of cancers and infectious diseases, as well as the use of alternative materials for the nanoparticle core, were studied in subsequent RBC membrane coating studies.<sup>100,101</sup> Membrane coating has also been accomplished using ultrasonic energy and microfluidic instruments in addition to physical extrusion.<sup>29,30</sup> This success cleared the path for biomimetic nanomedicine to be developed utilizing cell membranes obtained from other cells.<sup>97</sup>

Many attempts have been made in the design of chemotherapeutic to develop acceptable carriers for the co-delivery of chemotherapeutic and immunotherapeutic drugs with distinct physicochemical characteristics and modes of action. Furthermore, fast drug release at the tumor location with low drug degradation is required to provide an immediate anti-cancer impact. According to Shang *et al.*, a cancer cell membrane-cloaked pH-sensitive nanogel (NG@M) was reported to co-deliver paclitaxel (PTX) and the immunotherapeutic drug interleukin-2 (IL-2) for triple-negative breast cancer therapy. The charge reversible polymer rendered the nanogels with outstanding drug-loading ability and fast responsive drug-release behavior in the acidic tumor microenvironment. NG@M displayed 4.59-fold greater accumulation at the homologous tumor location. The rapidly released PTX and IL-2 improved dendritic cell development and stimulated the immune reaction *in situ*, as shown in Fig. 8. Enhanced anticancer activity and effective lung



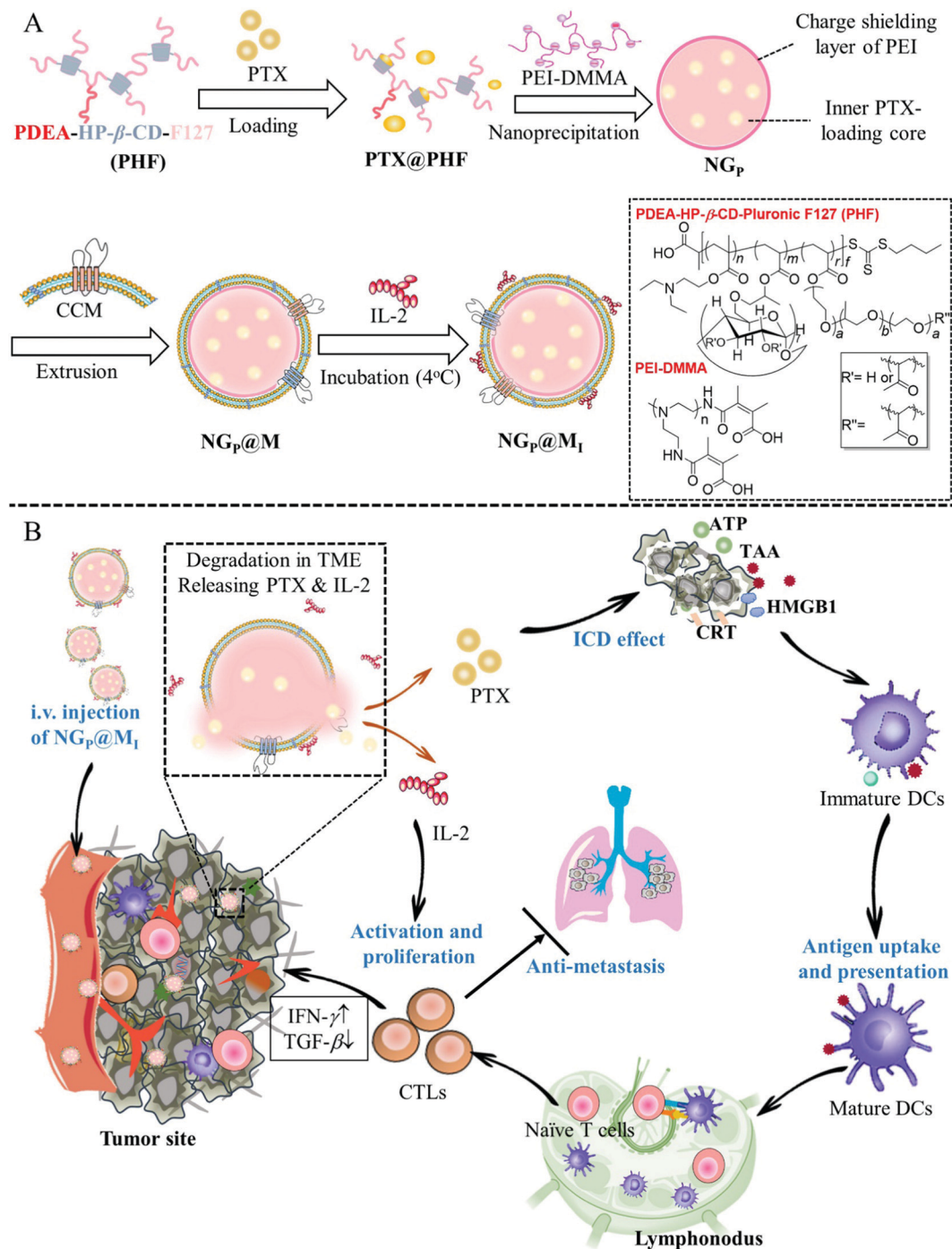


**Fig. 8** Schematic representation of NGP@MI used for cancer immunotherapy. (A) Formulation of NGP@MI. (B) Biodistribution, pH-responsive drug release and mechanism of NGP@MI for cancer immunotherapy against TNBC. Reproduced with permission.<sup>102</sup> Copyright 2021, Elsevier.

metastasis suppression were obtained with a longer median survival rate (39 days).<sup>102</sup>

As a novel delivery strategy for insoluble medicines, nanosuspension-based nanomedicine simply consists of a drug and a tiny amount of stabiliser distributed in an aqueous solution with a high drug content, narrow size distribution, high dispersal, and large surface area. For instance, the solubility, bioavailability, and effectiveness can all be considerably improved.

Fan *et al.* used an ultrasonic precipitation approach to make paclitaxel nanosuspensions ((PTX)NS), with a glioma C6 cancer cell membrane (CCM) coating and modified with DWSW peptide, which exhibited BBB penetration and tumour targeting capabilities *via* a homologous targeting mechanism. These findings demonstrated that the cancer cell membrane could successfully conceal the nanosuspension, preventing it from being cleared by the immune system and allowing them to pass through the



blood–brain barrier (BBB) and target tumour tissues preferentially. The absorption of the nanosuspension by tumour cells and its distribution in cerebral gliomas increased. DWSW-CCM-(PTX)NS inhibited the development of glioma cells and significantly extended the survival time of glioma-bearing mice. The coating also gave the nanosuspension biological features such as homologous adhesion and immune evasion, as illustrated in Fig. 9. This research offers a comprehensive strategy for increasing nanosuspension targeting and highlights the high application of biomimetic nanosuspensions for tumour treatment.<sup>103</sup>

### 4.3 PTX-loaded polymeric nanoparticles

Nanomedicine of PTX with polymers is a novel method that enhances its bioavailability and lowers the incidence of adverse effects. Many natural and synthetic polymers have been used for PTX nanoencapsulation, including PLGA NPs, PLA NPs, chitosan NPs and polymeric micelles, which are discussed here in detail. The general properties of these polymers include biocompatibility, easy manipulation of their physicochemical properties, biodegradability, and modulated drug release, as shown in Table 1.<sup>104</sup>

**4.3.1 Poly(lactic-co-glycolic acid) nanoparticles (PLGA NPs).** A commonly utilized biodegradable copolymer in nanoformulations is PLGA, which is hydrolyzed inside the body into the safe and non-toxic metabolites lactic and glycolic acid, eventually producing water and CO<sub>2</sub>.<sup>111</sup> The systemic toxicity with these two main metabolites is minimal because they are efficiently cleared from the body.<sup>112</sup>

PLGA nanoparticles loaded with PTX have been formulated using various methods such as oil-in-water emulsion solvent evaporation,<sup>113,114</sup> nanoprecipitation<sup>115</sup> and interfacial deposition methods.<sup>116</sup> Generally, paclitaxel was released from the nanoparticles in a biphasic pattern, consisting of a rapid initial release rate over 1 to 3 days, followed by a slow, sustained release.<sup>83</sup> These nanoparticles were shown to exhibit greater *in vitro* cytotoxicity than free paclitaxel in many tumors cell lines, such as glioma C6 cells,<sup>117</sup> human small cell lung cancer<sup>115</sup> and HeLa cells.<sup>115,116</sup> The *in vivo* tumor inhibitory activity of paclitaxel-loaded nanoparticles was markedly better in transplantable liver tumors.<sup>118</sup> The surface modification of nanoparticles led to improved paclitaxel delivery. This was achieved by B. Faraji Dizaji *et al.* by integrating zeolites into nanofibers for attaining the controlled

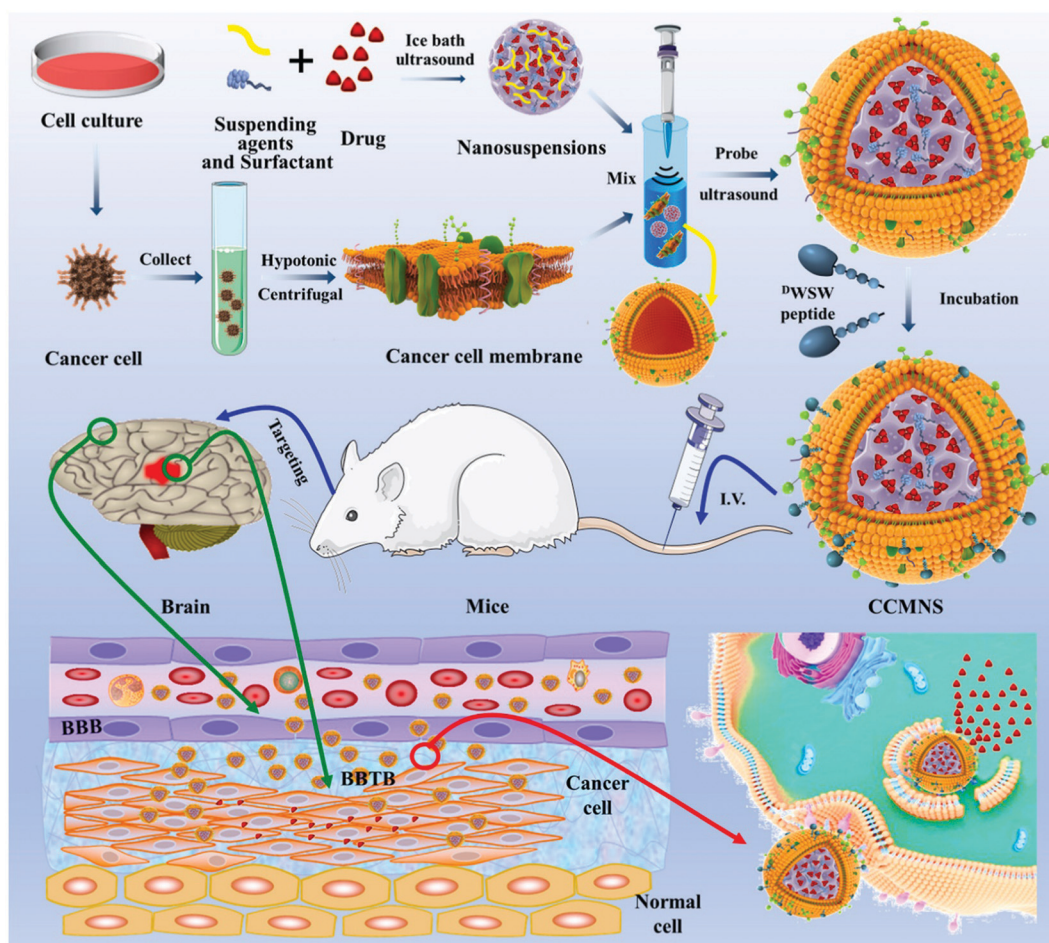


Fig. 9 Representation of biomimetic nanosuspension. This diagram illustrates the preparation of nanoparticles and their coating with a biomimetic membrane, ligand modification over the biomimetic membrane via lipid insertion and evaluation of its *in vivo* anti-tumor effect. Reproduced with permission.<sup>103</sup> Copyright 2021, Elsevier.



**Table 1** Essential characteristics of the polymeric nanoparticles used to deliver PTX in cancer therapy

Characteristics	Detail	Ref.
Biocompatibility	There should not be an induction of inflammation or carcinogenesis in the host's body. The material or its metabolites should not be toxic to the host cells.	105
Biodegradability	The material must decompose without producing any harmful metabolites or residues.	106
Stability	Chemical and mechanical stability is important to preserve the functions of the material.	107
Interactions with cells	The material should utilize specific surface charges and other properties to ensure improved and targeted cell adhesion. This depends on its structure and physicochemical properties.	108
Processability	The synthesis of the material should be simple, feasible and not demand advanced techniques.	109
Sustained release of drug	The material should be capable of sustained release of the drug.	110

release of paclitaxel *in vitro* and *in vivo*. The examples of zeolites used include hydrophilic Y zeolite, metal-organic frameworks, and hydrophobic ZSM 5 zeolites.<sup>119</sup> Nanobubbles (NBs) targeting cancer were designed by M. Wu *et al.* by using A10-3.2 aptamers targeted against PSMA or -specific membrane antigen and paclitaxel was concentrated in them.<sup>120</sup> This research group also investigated their effect on the ultrasound and treatment regimen of cancer. Water/oil/water double emulsion and carbodiimide methods were used to formulate the PTX-A10-3.2-PLGA nanobubbles. The binding of these nanobubbles to PSMA-positive LNCaP cells was confirmed using flow cytometry coupled with fluorescence imaging. It was believed that these nanobubbles have a long transit time and travel for long enough to target cancer cells.<sup>121</sup> It was also speculated that paclitaxel was released at a sustained rate owing to the enhanced permeability and retention impact. The results showed that these nanobubbles led to a greater drug release using only low-frequency ultrasound. The inhibitory concentration was also much lower and according to the *in vitro* evaluation, and efficient programmed cell death occurred (apoptosis).<sup>122,123</sup> The best tumor inhibition rate was achieved when low-frequency ultrasound was combined with these nanobubbles in tumor xenografts in mice. The survival rate was improved with negligible toxic effects. To visualize the changes in the PTX-A10-3.2-PLGA and PTX-PLGA NB parameters, LNCaP xenografts in mice were employed. In the live small animals, laser confocal scanning microscopy and fluorescence imaging showed the location of the fluorescence-labeled paclitaxel-A10-3.2-PLGA and nanobubbles. The results showed that in contrast mode and fluorescence imaging, the nanobubbles had high gray-scale intensity and their ability to aggregate also increased.<sup>124</sup> To conclude their findings, an A10-3.2 aptamer and

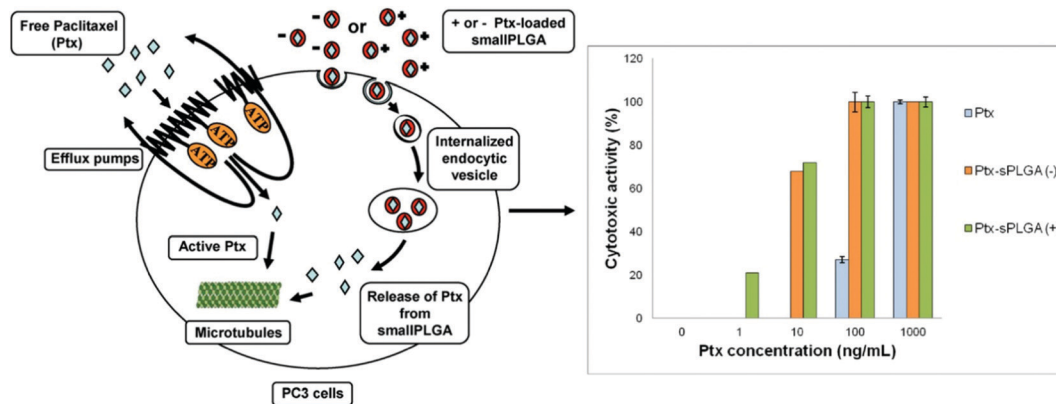
loaded PTX-PLGA multifunctional theranostic agent was synthesized for the ultrasound imaging of cancer, which was also used as therapy.<sup>125</sup> D. Le Broc-Ryckewaert *et al.* formulated nanoparticles loaded with paclitaxel with a size in the range of 49–95 nm together with charged surfaces, which were synthesized without the use of any surfactant or detergent. HPLC was used to determine their high stability with high PTX loading. Flow cytometry was used to evaluate the intake of the drug by PC3 cells. It was also confirmed that a relatively low dose of these nanoparticles altered the tubulin structure in cells. This study indicated that the charged nanoparticles transported the drug into PC3 cells and the efficiency of paclitaxel increased two-fold. The significance of nanoformulations in cancer therapy and their potential in *in vivo* applications are highlighted in Fig. 10.<sup>126</sup>

Due to the poor distribution of IV-administered chemotherapeutics to the bone, the advanced stage of cancer with bone metastases is very difficult to treat. I. M. Adjei *et al.* altered the composition and surface charge of biodegradable nanoparticles to have a sustained circulation time in the blood and reduced their size to facilitate their extravasation through the sinusoidal capillaries of the bone. The surface charge was neutralized by manipulating the composition of the emulsifying agent. This neutrality made the nanoparticles better at concentrating in the bone marrow than nanoparticles that were either positively or negatively charged. These nanoparticles were both small in size, around 320 nm, and neutral. This delivery to metastasized sites was hypothesized to stop the cancer progression and lower bone loss. In an osteolytic intraosseous model pertaining to cancer, neutral and small nanoparticles were concentrated in greater amounts within the bone metastases

**Table 2** A summary of the different types of PTX nanomedicines used for targeted cancer therapy

Type of nanomedicine	Drug use	Preparation method	Treatment	Ref.
PLGA NPs	PTX	Nanoprecipitation	Lung, cervical and liver cancer	126
PLA NPs	PTX	Nanoprecipitation	Glioma	132
Chitosan NPs	PTX	Dialysis	Advanced prostate cancer	141
Polymeric Micelles	PTX	Self-assembly	Prostate and liver cancer	80 and 81
PTX-polymer conjugates	PTX	Through ester linker	Liver cancer	137
Gold NPs	PTX	Nanoprecipitation	Prostate cancer	141
Iron oxide NPs	PTX	Interfacial deposition	Lung and prostate cancer	143
Magnetic NPs	PTX	Solvent displacement	Head and neck cancer	142
Cyclodextrin NPs	PTX	Self-assembly	Ovarian and lung cancer	149
Carbon nanotubes	PTX	Self-assembly	Prostate cancer	144
Nanobubbles	PTX	Self-assembly	Lung and prostate cancer	152
Nanodisks	PTX	Self-assembly	Prostate cancer	154





Differently charged paclitaxel-loaded smallPLGA nanoparticles highly improve cytotoxic activity of Paclitaxel.

Fig. 10 Differently charged PTX-loaded small PLGA nanoparticles highly improve the cytotoxic activity of PTX against PC3 prostatic cancer cell lines. Reproduced with permission.<sup>126</sup> Copyright 2013, Elsevier.

than the contralateral bone. A single dose of these nanoparticles loaded with paclitaxel given intravenously delayed the process of bone metastasis. This neutral combination also showed much less bone loss than the Cremophor EL formulation, which causes weight loss, whereas no acute toxic effects were seen with neutral nanoparticles. This shows that by modulating the physical and release properties, treatment options can be explored to address bone metastasis.<sup>127</sup>

**4.3.2 Poly(lactide) nanoparticles (PLA NPs).** PLA is another widely used matrix material for the preparation of polymeric NPs because of its biodegradable and safe properties. Methoxy poly(ethylene glycol)-poly(lactide) co-polymer (mPEG-PLA) was synthesized and incorporated in NPs to provide long-circulating properties.<sup>128,129</sup> The *in vitro* cytotoxicity of these NPs increased by 33.3-fold compared to that of Taxol after 24 h in MCF-7 cells. *In vivo*, the pharmacokinetic studies demonstrated the AUC and half-life of the PTX mPEG-PLA NPs in rat plasma were 3.1- and 2.8-fold greater than that of Taxol, respectively.<sup>130,131</sup> Wang *et al.* developed novel NPs of star-like copolymer mannitol-functionalized poly(lactide)-vitamin E TPGS (M-PLA-TPGS) for the delivery of PTX for cancer treatment and evaluated their therapeutic effects in a cancer cell line and animal model in comparison with the linear PLGA NPs and poly(lactide)-vitamin E TPGS (PLA-TPGS) NPs. The PTX-loaded M-PLA-TPGS NPs, prepared by a modified nanoprecipitation method, were observed by FESEM to be near-spherical in shape with a narrow size distribution. The drug-loaded NPs were further characterized to determine their size, surface charge, drug content, encapsulation efficiency and *in vitro* drug release. The results showed that the M-PLA-TPGS NPs were stable, showing almost no change in particle size and surface charge during the three-month storage period. *In vitro* drug release exhibited a biphasic pattern with initial burst release followed by slow and continuous release. The cellular uptake level of the M-PLA-TPGS NPs was demonstrated to be higher than the linear PLGA NPs and PLA-TPGS NPs in PC-3 cells. The data also showed that the PTX-loaded M-PLA-TPGS nanoparticles have higher anti-tumor efficacy than linear PLA-TPGS nanoparticles and PLGA nanoparticles *in vitro* and *in vivo*.

In short, the star-like copolymer M-PLA-TPGS can be used as a potential and promising molecular biomaterial in developing novel nanomedicine for cancer treatment.<sup>132</sup>

**4.3.3 Chitosan nanoparticles.** Ma *et al.* succeeded at developing porous nanofibers made of chitosan using a combination of chitosan/polyethylene oxide (PEO) and electrospinning, followed by dehydration. Scanning electron microscopy was used to observe their porous morphological features.<sup>133</sup> To load the drug, the nanofibers were submerged in a 0.1% w/w solution of paclitaxel. Then, the porous chitosan nanofibers were immersed in a 4% w/w solution of hyaluronic acid of polyanion nature for encapsulation. The subsequent interaction between these two was evaluated using FT-IR (Fourier transform infrared spectroscopy) and DSC (differential scanning calorimetry). UV-visible spectroscopy was used to analyze the paclitaxel release from the encapsulated fibers in PBS. MTT was used to check the *in vitro* DU145 cancer cell activities pertaining to the encapsulated nanofibers. The cell culture results revealed that the paclitaxel-loaded nanofiber mats had significant anti-cell attachment and anti-proliferation activity. This data strongly supports the idea that the chitosan/hyaluronic acid fibers modulated the release rate of paclitaxel and can be potentially used in post-op chemotherapy.<sup>134</sup> The biodegradable poly(1,4-phenyleneacetone dimethylene thioketal) (PPADT) nanoparticles have emerged for the intracellular delivery of anticancer agents. These nanoparticles are chemically synthesized through a condensation polymerization reaction between 2,2-dimethoxypropane and 1,4-benzenedimethanethiol. This is followed by encapsulation of the resulting PPADT with Nile red or paclitaxel. Reactive oxygen species provides a conducive environment for the polymer degradation by cleaving the thioketal bonds, which distorts the nanoparticles, releasing the encapsulated moiety. PC-3 cancer cells were used to evaluate the therapeutic efficacy of these paclitaxel-loaded PPADT nanoparticles, while the placebo PPADT nanoparticles do not lead to severe cytotoxicity. In conclusion, this study hinted at the potential use of ROS-sensitive biodegradable PPADT nanoparticles to intracellularly deliver insoluble therapeutic agents.<sup>135</sup>



#### 4.4 Development of PTX-polymer conjugates

Concomitant chemotherapy often fails to owing to the presence of CSCs or cancer stem cells and the drug resistance induced in tumors due to the changed expression of microRNAs.<sup>136</sup> This alteration occurs because of distorted signaling pathways such as Hedgehog (Hh) signaling. Yang *MS et al.* showed that paclitaxel, in combination with the Hh inhibitor cyclopamine (CYP) targets cells that are resistant to the drug. A portion of cells abundant in cancer stem cells, known as the side population, is also inhibited. They formulated PTX-polymer conjugates of mPEG-*b*-PCC-*g*-PTX-*g*-DC (P-PTX) and mPEG-*b*-PCC-*g*-CYP-*g*-DC (P-CYP), which turned into micelles. This combination helped combat the drug resistance to paclitaxel and also inhibited the colony formation in tumors. This combination also targeted the Hh signaling and stimulated the upregulation of the tumor suppressor miRNAs. In nude mice in which an orthotopic tumor was induced, this combination of P-PTX and P-CYP could inhibit the tumor growth compared to single therapy. In analyzing the

tumor cryosections immunohistochemically, using staining (H&E and Ki-67) and the TUNEL assay, it was established that this combination under testing could be used to address tumor resistance to chemotherapeutics, as illustrated in (Fig. 11).<sup>137</sup>

#### 4.5 Inorganic nanoparticles

**4.5.1 Gold nanoparticles.** Lately, siRNA, also known as small interfering RNA, has been explored for its therapeutic use for malignant disorders. However, its clinical utilization has been hindered by the lack of efficient means for its delivery.<sup>138,139</sup> Recently, multifunctional gold nanoparticles (AuNPs) have been studied as non-viral vectors for moving anticancer agents, proteins, peptides and genes.<sup>140</sup> Luan *et al.* used polyethylenimine (PEI) and PEGylated anisamide (a ligand known to target the Sigma receptor) to cap these gold nanoparticles to yield cationic anisamide-targeted PEGylated gold particles. Electrostatically, the nanoparticles targeted at anisamide formed a complex with siRNA and produced a complex with the

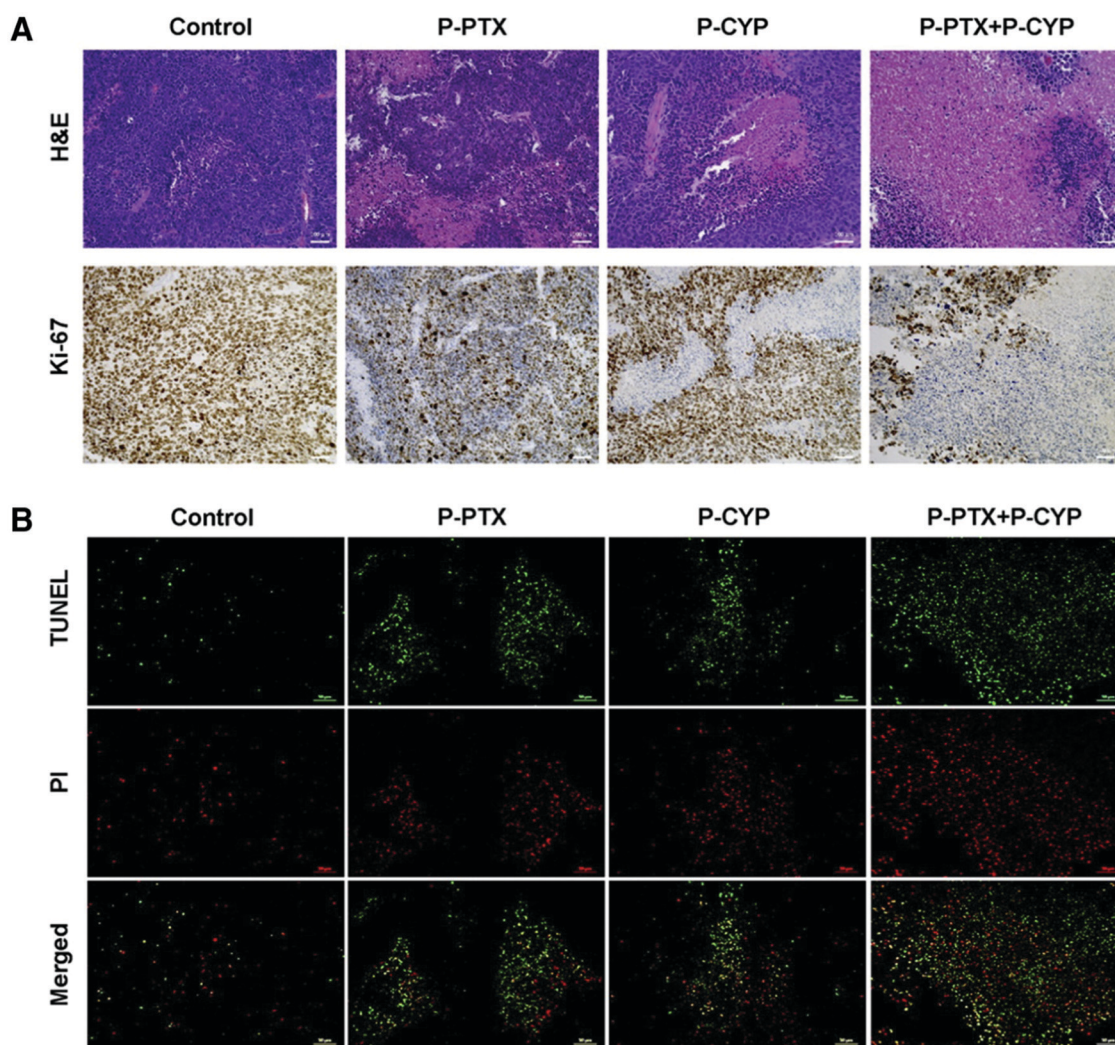


**Fig. 11** (A) Using TUNEL assay, H&E staining and Ki-67 (cell proliferation marker), the tumor samples were examined. Using saline as the control, the P-PTX, P-CYP and P-PTX + P-CYP treated tumor samples were removed and treated with H&E and Ki-67 staining. (B) The samples also underwent staining for green TUNEL-positive nuclei and red propidium iodide-positive nuclei. Reproduced with permission.<sup>137</sup> Copyright 2017, Elsevier.



desired physicochemical properties such as surface charge, size and stability. The complex was termed Au110-PEI-PEG5000-AA siRNA. These anisamide-targeting gold particles acted on human cancer cells *in vitro*, which helped the siRNA move out of the endosome. This also downregulated the RelA gene. Using the anisamide-targeted nanoparticles, a longer exposure of the small interfering RNA was achieved, which inhibited the cancer proliferation in a PC3 xenograft mouse model with no aggravated toxic effects. Another synergism was observed when combining siRNA-mediated NF- $\kappa$ B knockdown incorporating anisamide-targeted gold particles with paclitaxel for use in cancer treatment.<sup>141</sup>

**4.5.2 Magnetic nanoparticles.** Hua *et al.* developed a harmless drug nanocarrier consisting of carboxyl groups using magnetic nanoparticles (MNPs) of Fe<sub>3</sub>O<sub>4</sub> together with the hydrophilic polyaniline derivative poly[aniline-*co*-sodium *N*-(1-one-butyric acid) aniline] (SPANa), followed by soaking in an aqueous solution of HCl to synthesize SPANH/MNPs shell/core. These could also be employed to concentrate the hydrophobic paclitaxel. This improved the thermal stability and water solubility of the drug. One mg of SPANH/MNPs could sap 302.75  $\mu$ g of paclitaxel. At 25 °C and 37 °C, the bound-PTX showed higher stability and cytotoxicity than the free form. Upon the use of magnetic targeting, cellular inhibition was enhanced. This study showed that more efficacious cancer treatment is achieved using magnetic targeted delivery, which needs a lower drug dose and causes fewer adverse effects, as depicted in Fig. 12.<sup>142</sup>

Similarly, Ahmed *et al.* developed LHRH-AE105-IONPs to deliver drugs in advanced cancer and lower the incidence of side effects of chemotherapy. This multifunctional double-receptor-targeting iron oxide nanoparticles (IONPs) (luteinizing hormone-releasing hormone receptor [LHRH-R] peptide- and

urokinase-type plasminogen activator receptor [uPAR] peptide-targeted iron oxide nanoparticles) were led by two peptides, targeting the LHRH-receptor and uPAR on cancer cells, which guided the drug delivery towards the tumor site. The hydrodynamic size of these nanoparticles is larger compared to the non-targeted ones (NT-IONPs), which was measured *via* dynamic light scattering. The zeta potential of the drug-loaded nanoparticles was measured using surface analysis. Adequate internalization of the LHRH-AE105-IO nanoparticles by the human cancer line-3 was seen using Prussian blue staining. The nanoparticles concentrated in and were bound to the PC-3 cells rather than healthy epithelial cells (RC77N/E), which was determined *in vitro* using MRI. Upon uptake by the PC-3 cells, the nanoparticles sustained T<sub>2</sub> MRI contrast effects and low T<sub>2</sub> values. They were also successful at reducing the viability of the cancer cell line (PC-3) compared to NT-IO nanoparticles.<sup>143</sup>

#### 4.6. Development of PTX-carbon nanotubes

Recently, the integration of PTX in multi-wall carbon nanotubes (CNTs) in association with polyethyleneimine was reported. Then antibodies against PSMA were used to coat or cover the nanotubes to target cancer cells. Then, the fluorescent CNT composites were exposed to PSMA positive PCa cells, CaCo-2 colon cancer cells (PSMA-), HCT-116 and PSMA negative monocytes and lymphocytes *in vitro*. The cell-composite interaction was studied using flow cytometry and fluorescence microscopy. The results were visualized, indicating a slight interaction between the CNTs, CNT-PTX and the cells. Compared to paclitaxel or CNTs alone, the cancer (PSMA+) and colorectal cancer cells (PSMA negative) had greater sensitivity to the complex of paclitaxel with CNTs. Simultaneously, the incorporation of anti-PSMA (CNT-PTX-PSMA) improved the toxicity on LNCaP cells but not on the PSMA

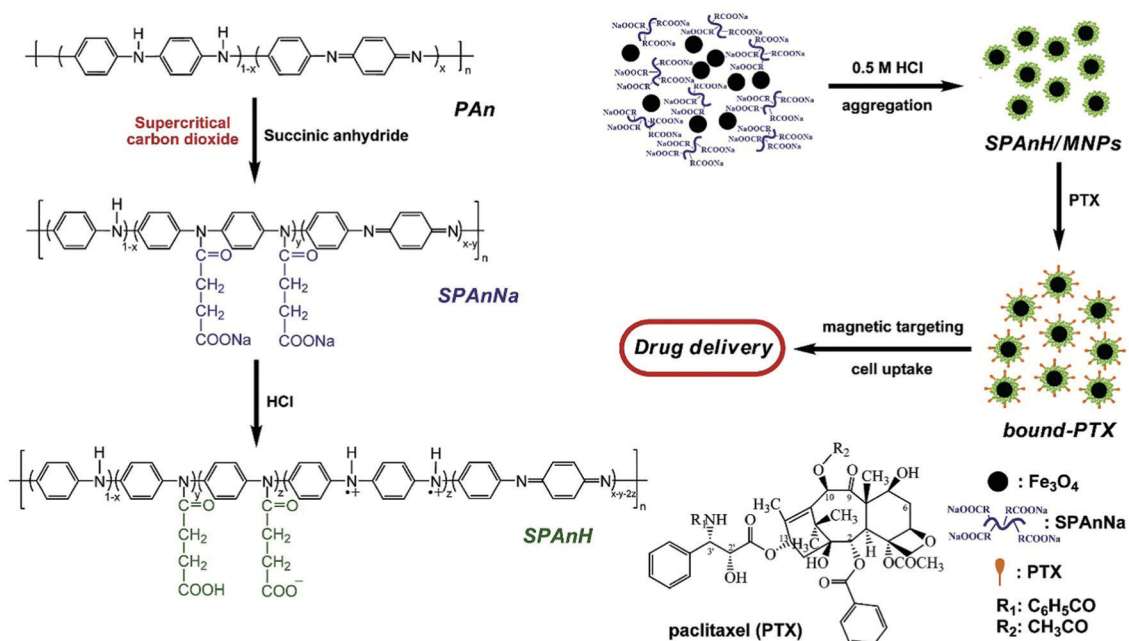


Fig. 12 Schematic illustrating the synthesis of the bound paclitaxel. Reproduced with permission.<sup>142</sup> Copyright 2010, Elsevier.



targets. No toxicity was observed in human monocytes and lymphocytes, but the composites induced phenotypical changes in monocytes. Thus, these results demonstrate the feasibility of using anti-PSMA antibodies to deliver drug-loaded CNTs to cancer cells as a strategy for improving the effectiveness of antineoplastic agents, as shown in Fig. 13.<sup>129</sup>

#### 4.7 Others

As a first-line agent to treat cancer, paclitaxel is widely used, but the associated drug resistance is very common despite the short treatment course. Guo *et al.* used PTX-resistant LNCaP (LNCaP/PTX) cells and found that they exhibited an EMT transition together with metastasis. They found that the expressions of  $\beta$ -tubulin III, androgen receptor, and CXCR4 were markedly high in the LNCaP/PTX cells, which play a central role in the development of resistance. Thus, to alleviate the drug resistance, core-shell nanoparticles of PSMA aptamer were synthesized. The inner core consisted of DSPR with paclitaxel and the outer shell consisted of Apt-PEG2K and siRNAs, which absorb calcium phosphate. This led to the sustained release of the siRNA and paclitaxel. The concentrated siRNA was slowly released into the cytoplasm when CaP stimulated its escape. This movement helped reverse EMT and improve the sensitivity of the cells towards paclitaxel. The slow release of the drug from the core helped enhance the effect of chemotherapy. As depicted in Fig. 14, this combination of PTX/siRNA NP-Apt showed good targeting of the tumor, and the subcutaneous and

orthotopic cancer model showed improved effectiveness with negligible side-effects.<sup>145</sup>

**4.7.1 Cyclodextrin (CD) nanoparticles.** The most common approach to treat metastatic cancer is the use of cytotoxic anticancer agents. However, the major downside of this regimen is the poor aqueous solubility and efficiency of these agents.<sup>146,147</sup> Examples of medicinal compounds with these issues include curcumin and paclitaxel. Boztas *et al.* made a novel system, where curcumin and paclitaxel were encapsulated in poly( $\beta$ -cyclodextrin triazine) or PCDT. This was tested in ovarian, lung and breast cancer models. Complexation increased the cytotoxicity and the drug-induced apoptosis of paclitaxel also. These Annexin V studies on the paclitaxel-induced apoptosis were carried out in the human ovarian cancer cell lines A2780 and SKOV-3, human non-small cell lung carcinoma cell line H1299, and human cancer line DU-145. However, no striking effect was seen with the complexation of paclitaxel and PCDT. Upon investigation of the bioactivity of the two compounds, the synergistic relationship was revealed, especially when complex formation occurred with PCDT on A2780, SKOV-3, and H1299 cancer cell lines.<sup>148</sup>

Based on the host and guest interaction, Pei *et al.* designed reliable supramolecular binary vesicles between  $\beta$ -cyclodextrins ( $\beta$ -CDs) and paclitaxel dimer. The two techniques employed to evaluate the inclusion complexation between the paclitaxel dimer and  $\beta$ -CDs in water were <sup>1</sup>HNMR spectroscopy and 2D rotating-frame Overhauser effect spectroscopy. The resultant amphiphilic complexes were capable of assembling into

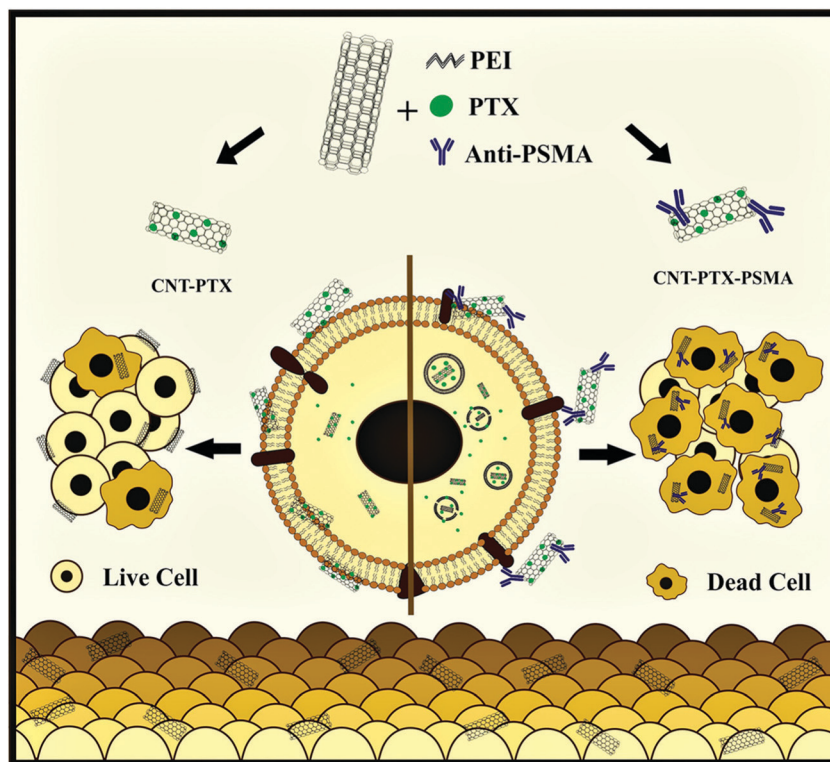
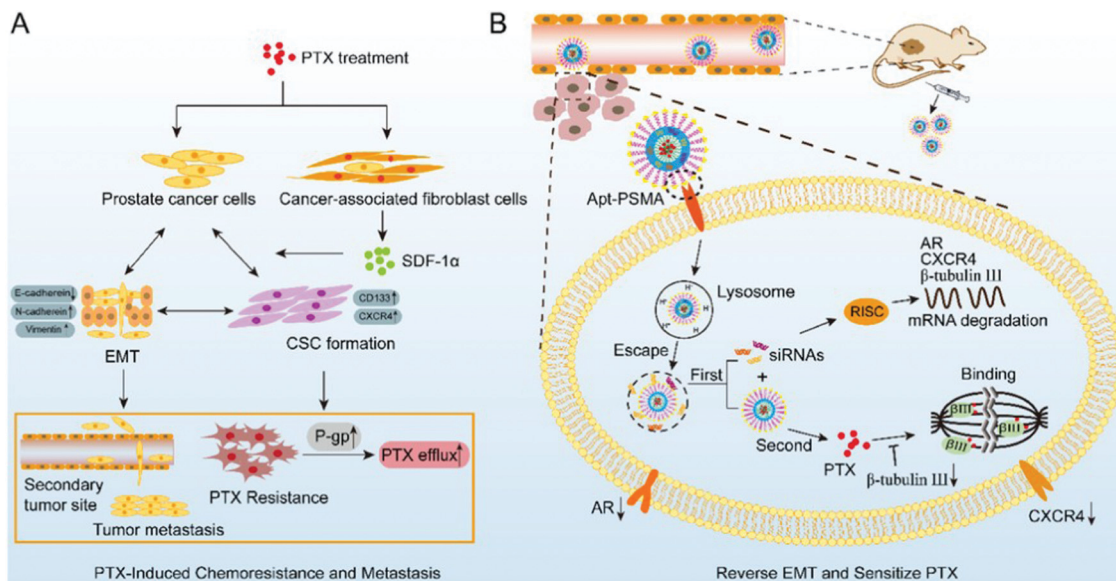


Fig. 13 Schematic showing the use of multiwall carbon nanotubes in conjunction with monoclonal antibodies targeted against PSMA and loaded with PTX to treat cancer cells. Reproduced with permission.<sup>144</sup> Copyright 2020, Elsevier.







**Fig. 14** Paclitaxel resistance and metastasis of cancer were tackled when aptamer-functionalized core-shell nanoparticles intermittently released the concentrated siRNAs and paclitaxel. (A) EMT stimulated during paclitaxel chemotherapy plays a role in the development of drug resistance to paclitaxel and PCa metastasis. (B) Metastasis can be halted and the sensitization of PCa cells to paclitaxel can be achieved by using PTX/siRNA NP-Apt to reverse the process of EMT. Reproduced with permission.<sup>145</sup> Copyright 2019, the American Chemical Society.

230 nm-wide vesicles by themselves. Using  $\alpha$ -amylase to break down the  $\beta$ -CDs or incorporating amantadine HCl, these vesicles could reversibly turn into nanoparticles. The reversal required the use of sufficient  $\beta$ -CDs again. These vesicles were also investigated to load the hydrophilic dye indocyanine or doxorubicin, a hydrophobic chemotherapeutic agent. The goal was to obtain the controlled release of these drugs when stimulated externally. Consequently, prodrugs can be used as starting materials to create supramolecular systems, as shown in Fig. 15.<sup>149</sup>

To improve the solubility of water-insoluble drugs, keep them safe from degradative processes and have a sustained release, beta-cyclodextrins ( $\beta$ -CD) are used to modify the substances used in drug delivery. Local delivery of PTX *via* alginate polysaccharide of a natural origin was achieved with  $\beta$ -CyD-moieties by Aanerud Omtvedt *et al.*, who developed a drug delivery method based on hydrogels. Due to its formation of an inclusion complex with CD, PTX was employed.<sup>150</sup> The resulting hydrogels were characterized for their mechanical and rheological properties, *in vitro* anticancer effect on PC-3 PCa cells and drug release *in vitro*. The mechanical properties of the hydrogels were reduced upon the addition of  $\beta$ -CyD-moieties compared to the unmodified sample, but the kinetics of gelatin did not vary much. The modified gels also underwent crystallization less frequently, which eased the diffusion of the drug out of the gel. Relative to the free HPP $\beta$ -CyD, the  $\beta$ -CyD-grafted alginate could more easily form a complex with PTX. The degradation products and PTX were released from the gel and had cytotoxic activity on cancer cells or PC-3 cells. This study hinted at the possible use of functionalized alginate with  $\beta$ -CyDs for delivering chemotherapeutics to cancer cells.<sup>151</sup>

**4.7.2 PTX-nanobubbles.** To get detailed tissue imaging with high contrast and excellent resolution, ultrasound is used

in conjunction with photoacoustic imaging, which efficiently measures and tracks cancer proliferation and metastasis. A productive method to deliver drugs is the use of UTND or ultrasound-targeted nanobubble destruction, which concentrates drugs in cancer cells and lowers the risk of side effects and can potentially be included in treatment.<sup>152</sup> Multifunctional nanobubbles loaded with indocyanine green and paclitaxel, which were denoted as ICG-PTX NBs, were synthesized by Lan *et al.* Other aspects studied were their use in ultrasound imaging and treatment of PCa together with UTND. The methodology utilized for formulating these nanobubbles was mechanical oscillation.<sup>105</sup> The particles size was in the range of  $469.5 \pm 32.87$  nm, and the zeta potential was  $-21.70 \pm 1.22$  mV. The efficiency of encapsulation was 68%, while the drug loading efficiency was 2.52%. It was also shown that these nanobubbles are compliant with ultrasound, fluorescence and photoacoustic imaging and the quality depends on their concentration. According to the tumor xenografts, these nanobubbles were suitable for multimodal imaging.<sup>152</sup> The ICG-PTX NB + US group had a stronger tumor inhibitory action on cancer proliferation and stimulation of apoptosis when tested both *in vitro* and *in vivo* in cancer cells and tumor xenografts ( $P < 0.05$ ). The AST, ALT, serum creatinine and BUN levels in the 6 groups were lower in the nanobubble group with  $P < 0.05$ .<sup>152</sup>

Upon H&E staining of the tissue, there was no evidence of conspicuous toxic effects in the ICG-PTX NB and the ICG-PTX NB + US groups. These nanobubbles are safer and can be used as pro-apoptotic contrast agents for the imaging techniques previously mentioned. Thus, they are promising in the treatment and diagnosis of cancer.<sup>152</sup>

**4.7.3 PTX-nanodisks.** Prostate cancer is the most common cancer in men, and chemotherapeutics is usually important



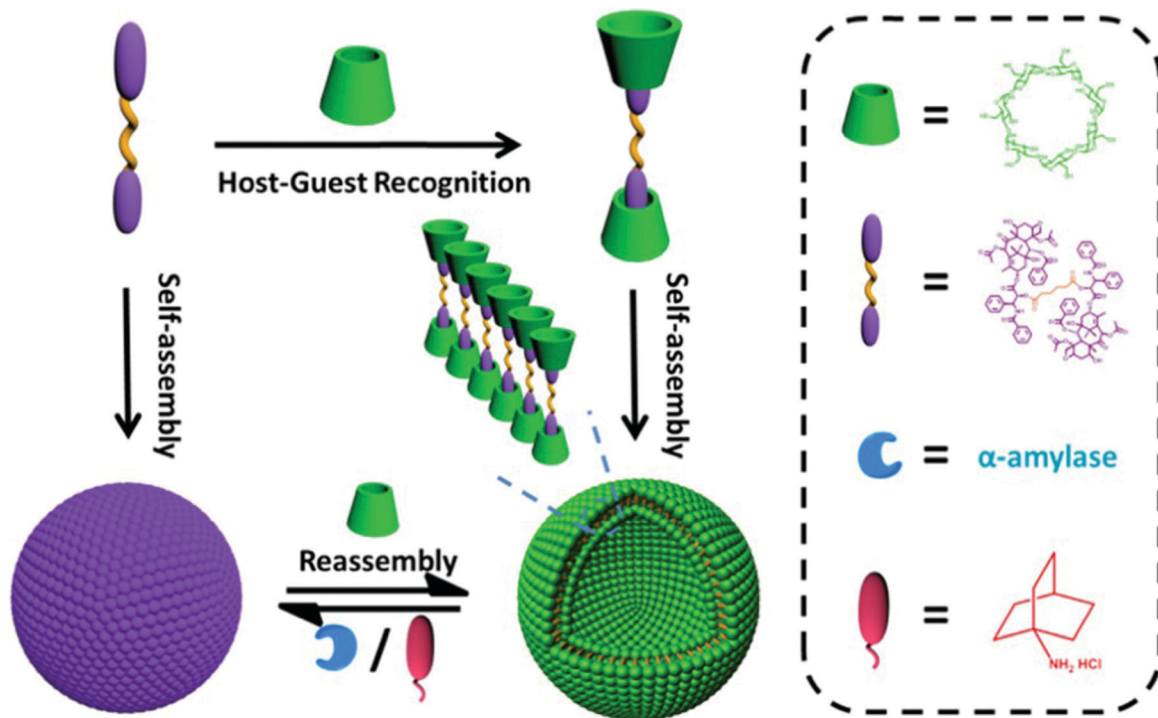


Fig. 15 Paclitaxel dimer and CD complexation, formation of supramolecular vesicles, and the reversible structure transformation between the dual-stimulus-induced NPs and vesicles. The dual stimulus consists of  $\alpha$ -amylase and adamantamine hydrochloride (AD). Reproduced with permission.<sup>149</sup> Copyright 2017, the American Chemical Society.

when this type of cancer is advanced.<sup>153</sup> Chemotherapy is associated with many side effects because of the non-targeted action and poor tissue concentration of drugs. Wang *et al.* formulated novel non-spherical nanodisks to explore the recent findings that unconventional non-spherical nanoparticles led to more drug retention and better tissue concentration than the conventional spherical ones. The nanodisks mentioned above were also modified using the targeting peptide CR(NMe)EKA to identify ECM fibronectin and the associated complexes in the tumor vessel walls and stroma. This increased their tumor-targeting activity. The nanodisks also increased the concentration of chemotherapeutics at the target site compared to conventional nanospheres. The CR(NMe)EKA-modified nanodisks containing paclitaxel also had improved anticancer activity compared to the free drug, nanospheres and simple or unmodified nanodisks. Thus, this study presented a new strategy to target PCa, with moderate preparation, enhanced efficiency, and reduced toxicity. It also supports the use of variably shaped nanoplatforms in therapeutics. Furthermore, it shared data to elucidate the biological effects of non-spherical nanodisks and compare how useful unconventional and novel nanoparticles are in therapeutics.<sup>154</sup>

## 5. Nanotoxicity of PTX nanomedicine and its consideration in clinical applications

For clinical applications, it is essential to understand the possible bio-interactions and *in vivo* results of PTX nanomedicine. In solid

tumors, elucidating the physiological properties and variations across existing models may be difficult, leading to low translation performance. Additional issues include unfavorable side effects, which necessitate more nanosafety considerations, particularly with almost all types of nanomedicine having health applications. Similarly, the regulatory framework, despite lacking in detail, can give further conceptual outlines and scientific prerequisites for the proper, safe, and scalable production of prospective PTX nanomedicine for cancer treatment.

PTX nanomedicines have different physicochemical properties, such as decreased size, increased surface area, chemical modification and adjustable properties, and high reactivity.<sup>155</sup> However, although these nanomaterials have obvious benefits in therapeutic systems and cancer treatment, they are not without limitations in terms of highly unsafe *in vivo* reactions. The variability and ambiguity of processes happening at the nanobio interfaces, and also the lack of understanding regarding the underlying toxicity effects of nanomaterials have delayed the authorization of nanoscale-designed products. The potential influence of PTX nanomedicine on health and the environment has attracted significant interest recently, spawning the subject of nanosafety as researchers work to better understand their characteristics and assess their nanotoxicological nature.<sup>156,157</sup> The ability to understand how PTX nanomedicine interacts with biological systems will become increasingly important in the future. Size, shape, surface coating, surface charge, physicochemical nature, stability, and degradability have all been identified as critical characteristics to investigate.<sup>158</sup> There is a distinct emphasis on inorganic nanoparticles, owing to the large number



of studies available on their potential toxicity compared to the limited studies available on polymer-based nanoparticles.<sup>159</sup> Machine-learning algorithms customized to anticipate *in vitro* nanotoxicology are indeed an intriguing platform that may have a significant influence on biosafety assessment in the coming years.<sup>160</sup> A proposal for a nanotoxicological categorization system based on two key factors, primarily nanomedicine diameter and biodegradability, has now been made.<sup>161</sup> Smaller PTX nanomedicine can be easily swallowed practically by all cell types in the body; however those larger than 100 nm have restricted internalization. Consequently, nanoparticles with a size less than 100 nm and non-biodegradable are classified as Class IV, while biodegradable nanoparticles with a size more than 100 nm are classified as Class I and regarded as the safest.

## 6. Challenges and future perspectives

Despite all the benefits and feasibility of nanoformulations, their application and use are limited because the characterization of their physicochemical properties is incomplete. Specifically, every nano-drug delivery method is different, which means that the scale-up of their manufacturing will also vary and pose a challenge. Another reason is that the knowledge about the stability of nanomedicine, their release and the elimination of their active moiety together with the vehicles *in vivo* is insufficient. It is now believed that metastasis or leakage of the tumor depends on the type of cancer. Also, the role of the EPR effect is still not concise. Thus, to better target tumors, it is desirable for particles to have a size of less than 40 nm. There is also a need to find new ligands that target the tumor to be modified, characterized, and induced in the targeted organs. There is also a need to study the toxic effects of nanoformulations in the long term. Therefore, the likelihood of using biodegradable and non-toxic polymers is greater owing to their low toxicity. Lastly, nanoformulations are expected to be very costly. However, their role and efficacy cannot be undermined and hold their potential to be used in cancer therapy.

## 7. Conclusion

Paclitaxel is a very productive chemotherapeutic agent, which is widely employed for the treatment of numerous malignancies. Currently, the formulation of paclitaxel used consists of Cremophor EL and ethanol, which has been reported to cause issues. Alternatively, the use of a nanoformulation of paclitaxel eliminates the need for these solvents, and hence lowers the associated side effects. The solubility and pharmacokinetic profile of paclitaxel also improve when it is employed as a nanoformulation. Furthermore, the EPR effect and targeted ligands are employed to work against the cancer cells. Therefore, nanotechnology is under heavy research both by clinical and industrial scientists and researcher in academia. Consequently, numerous types of nanomedicines of paclitaxel have emerged, as discussed in this review, including lipid-based formulations, polymer conjugates, polymeric, cyclodextrin and inorganic

nanoparticles, nanocrystals and carbon nanotubes. This review also presented the research on nanotechnology and paclitaxel nanoformulations to enhance the medical outcome of chemotherapy and cancer. Furthermore, we presented the novel and latest approaches developed pertaining to PTX nanoformulations that target the delivery of paclitaxel to cancer cells.

## Author contributions

Hajra Zafar, Faisal Raza and Muhammad Wasim Khan designed and wrote this review, Aftab Ullah, Asif Ullah Khan, Abdul Baseer, Rameesha Fareed and Muhammad Sohail put the individual parts together. Hajra Zafar and Faisal Raza, as corresponding authors, acquired the funding and reviewed, edited, and finalized this review.

## Conflicts of interest

The authors declare no conflict of interest.

## Acknowledgements

We are very thankful to the China Scholarship Council (CSC) and School of Pharmacy, Shanghai Jiao Tong University, China for their continuous support.

## Notes and references

- 1 X. Yu, M. Fallah, Y. Tian, T. Mukama, K. Sundquist, J. Sundquist, H. Brenner and E. Kharazmi, *Cancer*, 2020, **126**, 4371–4378.
- 2 S. Hema, S. Thambiraj and D. R. Shankaran, *J. Nanosci. Nanotechnol.*, 2018, **18**, 5171–5191.
- 3 M. M. Yallapu, P. K. Bhusetty Nagesh, M. Jaggi and S. C. Chauhan, *AAPS J.*, 2015, **17**, 1341–1356.
- 4 M. M. F. A. Baig, W.-F. Lai, A. Ahsan, M. Jabeen, M. A. Farooq, R. Mikrani, M. Abbas, M. Naveed, S. A. Kassim, F. Raza, A. A. Dar and M. T. Ansari, *Pharm. Res.*, 2020, **37**, 75.
- 5 S. Dombe and P. Shirote, *Curr. Drug Targets*, 2021, **22**, 443–462.
- 6 J. M. Guilford and J. M. Pezzuto, *Expert Opin. Invest. Drugs*, 2008, **17**, 1341–1352.
- 7 K. Asifullah, Z. Zhou, W. He, K. Gao, M. W. Khan, R. Faisal, H. Muhammad and M. J. M. P. Sun, *Mol. Pharmaceutics*, 2019, **16**, 2728–2741.
- 8 F. Raza, H. Zafar, Y. Zhu, Y. Ren, A. Ullah, A. U. Khan, X. He, H. Han, M. Aquib and K. O. Boakye-Yiadom, *Pharmaceutics*, 2018, **10**, 16.
- 9 F. Raza, Y. Zhu, L. Chen, X. You, J. Zhang, A. Khan, M. W. Khan, M. Hasnat, H. Zafar and J. Wu, *Biomater. Sci.*, 2019, **7**, 2023–2036.
- 10 Y. Zhu, L. Wang, Y. Li, Z. Huang, S. Luo, Y. He, H. Han, F. Raza, J. Wu and L. Ge, *Biomater. Sci.*, 2020, **8**, 5415–5426.
- 11 M. A. Jordan and L. Wilson, *Nat. Rev. Cancer*, 2004, **4**, 253–265.



- 12 M. Aquib, M. A. Farooq, P. Banerjee, F. Akhtar, M. S. Filli, K. O. Boakye-Yiadom, S. Kesse, F. Raza, M. B. Maviah and R. Mavlyanova, *J. Biomed. Mater. Res., Part A*, 2019, **107**, 2643–2666.
- 13 H. Gelderblom, J. Verweij, K. Nooter and A. Sparreboom, *Eur. J. Cancer*, 2001, **37**, 1590–1598.
- 14 P. Ma and R. J. Mumper, *J. Nanomed. Nanotechnol.*, 2013, **4**, 1000164.
- 15 Q. Chen, X. Liu, Z. Luo, S. Wang, J. Lin, Z. Xie, M. Li, C. Li, H. Cao, Q. Huang, J. Mao and B. Xu, *J. Cell Physiol.*, 2019, **234**, 6611–6623.
- 16 C. Rowbottom, A. Pietrasiewicz, T. Tuczewycz, R. Grater, D. Qiu, S. Kapadnis and P. Trapa, *Pharmacol. Res. Perspect.*, 2021, **9**, e00740.
- 17 M. W. Khan, P. Zhao, A. Khan, F. Raza, S. M. Raza, M. Sarfraz, Y. Chen, M. Li, T. Yang and X. Ma, *Int. J. Nanomed.*, 2019, **14**, 3753.
- 18 F. Raza, H. Zafar, X. You, A. Khan, J. Wu and L. Ge, *J. Mater. Chem. B*, 2019, **7**, 7639–7655.
- 19 A. Spader, J. Emami, F. Sanaee, M. Aminpour, I. M. Paiva, J. A. Tuszyński and A. Lavasanifar, *J. Pharm. Pharm. Sci.*, 2021, **24**, 344–362.
- 20 M. M. F. A. Baig, M. Sohail, A. A. Mirjat, M. Naveed, F. Majeed, F. Raza, M. A. Farooq, R. Mikrani, S. Khan and M. Abbas, *Appl. Nanosci.*, 2019, **9**, 2105–2115.
- 21 K. O. Boakye-Yiadom, S. Kesse, Y. Opoku-Damoah, M. S. Filli, M. Aquib, M. M. B. Joelle, M. A. Farooq, R. Mavlyanova, F. Raza and R. Bavi, *Int. J. Pharm.*, 2019, **564**, 308–317.
- 22 M. Hasnat, Z. Yuan, M. Naveed, A. Khan, F. Raza, D. Xu, A. Ullah, L. Sun, L. Zhang and Z. Jiang, *Cell Biol. Toxicol.*, 2019, **35**, 267–280.
- 23 M. Hasnat, Z. Yuan, A. Ullah, M. Naveed, F. Raza, M. M. F. A. Baig, A. Khan, D. Xu, Y. Su and L. Sun, *Toxicol. Mech. Methods*, 2020, **30**, 124–133.
- 24 G. Wei, Y. Wang, G. Yang, Y. Wang and R. Ju, *Theranostics*, 2021, **11**, 6370–6392.
- 25 A. Gülsu and M. C. Aslanpay, *Emerging Mater. Res.*, 2021, **10**, 321–328.
- 26 H. Zafar, F. Raza, S. Ma, Y. Wei, J. Zhang and Q. Shen, *Biomater. Sci.*, 2021, **9**, 5092–5115.
- 27 M. Barani, M. Bilal, F. Sabir, A. Rahdar and G. Z. Kyzas, *Life Sci.*, 2021, **266**, 118914.
- 28 A. S. Kymchenko, F. Liu, M. Collot and N. Anton, *Adv. Healthcare Mater.*, 2020, **10**, 2001289.
- 29 Y. Zhu, X. You, K. Huang, F. Raza, X. Lu, Y. Chen, A. Dhinakar, Y. Zhang, Y. Kang and J. J. N. Wu, *Nanotechnology*, 2018, **29**, 304001.
- 30 D. M. Anwar, M. El-Sayed, A. Reda, J.-Y. Fang, S. N. Khattab and A. O. Elzoghby, *Expert Opin. Drug Delivery*, 2021, **18**, 1609–1925.
- 31 S. Gao, X. Yang, J. Xu, N. Qiu and G. Zhai, *ACS Nano*, 2021, **15**, 12567–12603.
- 32 W.-H. Lee, C.-Y. Loo, P. M. Young, D. Traini, R. S. Mason and R. Rohanizadeh, *Expert Opin. Drug Delivery*, 2014, **11**, 1183–1201.
- 33 M. Aquib, H. Zhang, F. Raza, P. Banerjee, R. Bavi, S. Kesse, K. O. Boakye-Yiadom, M. S. Filli, M. A. Farooq and B. Wang, *J. Mol. Liq.*, 2022, **346**, 117065.
- 34 Y. Zhu, S. Luo, Y. Chen, F. Raza, H. Han, Z. Huang, Y. Li and L. Ge, *Mater. Express*, 2019, **9**, 831–838.
- 35 M. E. Davis, Z. Chen and D. M. Shin, in *Nanoscience and Technology*, ed. P. Rodgers, Nature Publishing Group, London, 2010.
- 36 P. Shadmani, B. Mehrafrooz, A. Montazeri and R. Naghadabadi, *J. Phys.: Condens. Matter*, 2020, **32**, 115101.
- 37 K. Amerigos Daddy J. C., M. Chen, F. Raza, Y. Xiao, Z. Su and Q. Ping, *Pharmaceutics*, 2020, **12**, 191.
- 38 R.-V. Kalaydina, K. Bajwa, B. Qorri, A. Decarlo and M. R. Szewczuk, *Int. J. Nanomed.*, 2018, **13**, 4727–4745.
- 39 A. Sparreboom, C. D. Scripture, V. Trieu, P. J. Williams, T. De, A. Yang, B. Beals, W. D. Figg, M. Hawkins and N. Desai, *Clin. Cancer Res.*, 2005, **11**, 4136–4143.
- 40 M. A. Lovich, C. Creel, K. Hong, C.-W. Hwang and E. R. Edelman, *J. Pharm. Sci.*, 2001, **90**, 1324–1335.
- 41 H. Zafar, M. H. Kiani, F. Raza, A. Rauf, I. Chaudhery, N. M. Ahmad, S. Akhtar and G. Shahnaz, *J. Nanopart. Res.*, 2020, **22**, 1–21.
- 42 A. Ullah, G. Chen, A. Hussain, H. Khan, A. Abbas, Z. Zhou, M. Shafiq, S. Ahmad, U. Ali, M. Usman, F. Raza, A. Ahmed, Z. Qiu, M. Zheng and D. Liu, *Int. J. Nanomed.*, 2021, **16**, 4451–4470.
- 43 E. Bernabeu, M. Cagel, E. Lagomarsino, M. Moretton and D. A. Chiappetta, *Int. J. Pharm.*, 2017, **526**, 474–495.
- 44 G. J. Fetterly and R. M. Straubinger, *AAPS PharmSci*, 2003, **5**, 32.
- 45 A. K. Singla, A. Garg and D. Aggarwal, *Int. J. Pharm.*, 2002, **235**, 179–192.
- 46 J. A. Zhang, G. Anyarambhatla and L. Ma, *et al.*, *Eur. J. Pharm. Biopharm.*, 2005, **59**, 117–187.
- 47 J. Zhai, F. H. Tan, R. B. Luwor, T. S. Reddi, N. Ahmed, C. J. Drummond and N. Tran, *ACS Appl. Bio Mater.*, 2020, **3**, 4198–4207.
- 48 H. Cai, X. Dai, X. Wang, P. Tan, L. Gu, Q. Luo, X. Zheng, Z. Li, H. Zhu, H. Zhang, Z. Gu, Q. Gong and K. Luo, *Adv. Sci.*, 2020, **7**, 1903243.
- 49 Q. Liu, D. Zhao, X. Zhu, H. Chen, Y. Yang, J. Xu, Q. Zhang, A. Fan, N. Li, C. Guo, Y. Kong, Y. Lu and X. Chen, *J. Pharm. Sci.*, 2017, **106**, 3066–3075.
- 50 J. Zhai, R. B. Luwor, N. Ahmed, R. Escalona, F. H. Tan, C. Fong, J. Ratcliffe, J. A. Scoble, C. J. Drummond and N. Tran, *ACS Appl. Mater. Interfaces*, 2018, **10**, 25174–25185.
- 51 J. Han, S. S. Davis, C. Papandreou, C. D. Melia and C. Washington, *Pharm. Res.*, 2004, **21**, 1573–1580.
- 52 S. Salehi, M. S. Nourbakhsh, M. Yousefpour, G. Rajabzadeh and S. Sahab-Nega, *J. Liposome Res.*, 2021, DOI: 10.1080/08982104.2021.2019763.
- 53 J. W. Singer, B. Baker, P. De Vries, A. Kumar, S. Shaffer, E. Vawter, M. Bolton and P. Garzone, *Adv. Exp. Med. Biol.*, 2003, **519**, 81–99.
- 54 J. Lim, A. Chouai, S.-T. Lo, W. Liu, X. Sun and E. E. Simanek, *Bioconjugate Chem.*, 2009, **20**, 2154–2161.



- 55 X. Wang, G. Zhao, S. Van, N. Jiang, L. Yu, D. Vera and S. B. Howell, *Pharmacology*, 2010, **65**, 515.
- 56 S. M. Basu, S. K. Yadava, R. Singh and J. Giri, *Colloids Surf., B*, 2021, **204**, 111775.
- 57 H. Chen, Y. Tang, H. Shang, X. Kong, R. Guo and W. Lin, *J. Mater. Chem. B*, 2017, **5**, 2436–2444.
- 58 J.-P. Nam, S.-C. Park, T.-H. Kim, J.-Y. Jang, C. Choi, M.-K. Jang and J.-W. Nah, *Int. J. Pharm.*, 2013, **457**, 124–135.
- 59 W. J. Trickler, A. A. Nagvekar and A. K. Dash, *AAPS PharmSciTech*, 2008, **9**, 486–493.
- 60 N. Erdoğan, G. Esendağlı, T. T. Nielsen, M. Şen, L. Öner and E. Bilensoy, *Int. J. Pharm.*, 2016, **509**, 375–390.
- 61 C. Yan, N. Liang, Q. Li, P. Yan and S. Sun, *Carbohydr. Polym.*, 2019, **216**, 129–139.
- 62 X. Lu, H. Wu, Y. Liang, Z. Zhang and H. Lv, *Int. J. Pharm.*, 2021, **600**, 120496.
- 63 L. Jia, J. Schweizer, Y. Wang, C. Cerna, H. Wong and M. Revilla, *Biochem. Pharmacol.*, 2003, **66**, 2193–2199.
- 64 J. Wang, M. Sui and W. Fan, *Curr. Drug Metab.*, 2010, **11**, 129–141.
- 65 X. Huang, Y. Li, D. Li, X. Zhou, H. Qiao, L. Yang, Y. Ji, X. Zhang, D. Huang and W. Chen, *Biomater. Sci.*, 2021, **9**, 6108–6115.
- 66 X. Pang, H.-L. Du, H.-Q. Zhang, Y.-J. Zhai and G.-X. Zhai, *Drug Discovery Today*, 2013, **18**, 1316–1322.
- 67 S. S. Suri, H. Fenniri and B. Singh, *J. Occup. Med. Toxicol.*, 2007, **2**, 1–6.
- 68 M. Knutson and M. Wessling-Resnick, *Crit. Rev. Biochem. Mol. Biol.*, 2003, **38**, 61–88.
- 69 F. Alexis, E. M. Pridgen, R. Langer and O. C. Farokhzad, *Handb. Exp. Pharmacol.*, 2010, **197**, 55–86.
- 70 G. Storm, S. O. Belliot, T. Daemen and D. D. Lasic, *Adv. Drug Delivery Rev.*, 1995, **17**, 31–48.
- 71 L. Shan, X. Zhuo, F. Zhang, Y. Dai, G. Zhu, B. C. Yung, W. Fan, K. Zhai, O. Jacobson, D. O. Kiesewetter, Y. Ma, G. Gao and X. Chen, *Theranostics*, 2018, **8**, 2018–2030.
- 72 R. K. Jain and T. Stylianopoulos, *Nat. Rev. Clin. Oncol.*, 2010, **7**, 653–664.
- 73 S. Mignani, J. Rodrigues, R. Roy, X. Shi, V. Ceña, S. El Kazzouli and J.-P. Majoral, *Drug Discovery Today*, 2019, **24**, 1184–1192.
- 74 B. Liu and S. Thayumanavan, *J. Am. Chem. Soc.*, 2017, **139**, 2306–2317.
- 75 H. Liu, H. Chen, F. Cao, D. Peng, W. Chen and C. Zhang, *Polymers*, 2019, **11**, 820.
- 76 H. Cao, Y. Xiang, Y. Zeng, Z. Li, X. Zheng, Q. Luo, H. Zhu, Q. Gong, Z. Gu, Y. Liu, H. Zhang and K. Luo, *Acta Pharm. Sin. B*, 2021, **11**, 544–559.
- 77 D.-C. Yang, S. Wang, X.-L. Weng, H.-X. Zhang, J.-Y. Liu and Z. Lin, *ACS Appl. Mater. Interfaces*, 2021, **13**, 33905–33914.
- 78 Z. Tang, L. Gao, J. Lin, C. Cai, Y. Yao, G. Guerin, X. Tian and S. Lin, *J. Am. Chem. Soc.*, 2021, **143**, 14684–14693.
- 79 C. C. Sproncken, J. R. Magana and I. K. Voets, *ACS Macro Lett.*, 2021, **10**, 167–179.
- 80 Y. Gao, Y. Li, Y. Li, L. Yuan, Y. Zhou, J. Li, L. Zhao, C. Zhang, X. Li and Y. Liu, *Nanoscale*, 2015, **7**, 597–612.
- 81 Y. Gao, Y. Zhou, L. Zhao, C. Zhang, Y. Li, J. Li, X. Li and Y. Liu, *Acta Biomater.*, 2015, **23**, 127–135.
- 82 A. W. Du, H. Lu and M. H. Stenzel, *Biomacromolecules*, 2015, **16**, 1470–1479.
- 83 D. Qu, M. Jiao, H. Lin, C. Tian, G. Qu, J. Xue, L. Xue, C. Ju and C. Zhang, *Carbohydr. Polym.*, 2020, **229**, 115498.
- 84 Y. Wang, L. Zhou, M. Xiao, Z.-L. Sun and C.-Y. Zhang, *Colloids Surf., B*, 2017, **149**, 16–22.
- 85 C. Zhu, H. Zhang, W. Li, L. Luo, X. Guo, Z. Wang, F. Kong, Q. Li, J. Yang, Y. Du and J. You, *Biomaterials*, 2018, **161**, 144–153.
- 86 Y. Zhou, H. Wen, L. Gu, J. Fu, J. Guo, L. Du, X. Zhou, X. Yu, Y. Huang and H. Wang, *J. Nanobiotechnol.*, 2017, **15**, 87.
- 87 Y. Zhu, X. Wang, J. Zhang, F. Meng, C. Deng, R. Cheng, J. Feijen and Z. Zhong, *J. Controlled Release*, 2017, **250**, 1–8.
- 88 J. Hu, G. Zhang and S. Liu, *Chem. Soc. Rev.*, 2012, **41**, 5933–5949.
- 89 Q. Zhou, L. Zhang, T. Yang and H. Wu, *Int. J. Nanomed.*, 2018, **13**, 2921–2942.
- 90 L. Wu, B. Lin, H. Yang, J. Chen, Z. Mao, W. Wang and C. Gao, *Acta Biomater.*, 2019, **86**, 363–372.
- 91 M. Egeblad and Z. Werb, *Nat. Rev. Cancer*, 2002, **2**, 161–174.
- 92 W. Ke, Z. Zha, J. F. Mukerabigwi, W. Chen, Y. Wang, C. He and Z. Ge, *Bioconjugate Chem.*, 2017, **28**, 2190–2198.
- 93 Q. Yao, Z. Dai, J. Hoon Choi, D. Kim and L. Zhu, *ACS Appl. Mater. Interfaces*, 2017, **9**, 32520–32533.
- 94 N. Hamasaki and M. Yamamoto, *Vox Sang.*, 2000, **79**, 191–197.
- 95 M. Holinstat, *Cancer Metastasis Rev.*, 2017, **36**, 195–198.
- 96 D. S. Vinay, E. P. Ryan, G. Pawelec, W. H. Talib, J. Stagg, E. Elkord, T. Lichtor, W. K. Decker, R. L. Whelan and H. S. Kumara, *Semin. Cancer Biol.*, 2015, **35**, S185–S198.
- 97 R. H. Fang, A. V. Kroll, W. Gao and L. Zhang, *Adv. Mater.*, 2018, **30**, 1706759.
- 98 F. Oroojalian, M. Beygi, B. Baradaran, A. Mokhtarzadeh and M.-A. Shahbazi, *Small*, 2021, **17**, 2006484.
- 99 P.-A. Oldenburg, A. Zheleznyak, Y.-F. Fang, C. F. Lagenaur, H. D. Gresham and F. P. Lindberg, *Science*, 2000, **288**, 2051–2054.
- 100 B. T. Luk, R. H. Fang, C.-M. J. Hu, J. A. Copp, S. Thamphiwatana, D. Dehaini, W. Gao, K. Zhang, S. Li and L. Zhang, *Theranostics*, 2016, **6**, 1004.
- 101 T. Escajadillo, J. Olson, B. T. Luk, L. Zhang and V. Nizet, *Front. Pharmacol.*, 2017, **8**, 477.
- 102 S. A. Ganai, F. A. Sheikh, Z. A. Baba, M. A. Mir, M. A. Mantoo and M. A. Yatoo, *Phytother. Res.*, **35**, 3509–3532.
- 103 Y. Fan, Y. Cui, W. Hao, M. Chen, Q. Liu, Y. Wang, M. Yang, Z. Li, W. Gong, S. Song, Y. Yang and C. Guo, *Bioact. Mater.*, 2021, **6**, 4402–4414.
- 104 R. Ferrari, M. Sponchioni, M. Morbidelli and D. Moscatelli, *Nanoscale*, 2018, **10**, 22701–22719.
- 105 R. Liao, J. Pon, M. Chungyoun and E. Nance, *Biomaterials*, 2020, **257**, 120238.
- 106 J. Karlsson, H. J. Vaughan and J. J. Green, *Annu. Rev. Chem. Biomol. Eng.*, 2018, **9**, 105–127.



- 107 W.-S. Cho, F. Thielbeer, R. Duffin, E. M. Johansson, I. L. Megson, W. MacNee, M. Bradley and K. J. N. Donaldson, *Nanotoxicology*, 2014, **8**, 202–211.
- 108 C. J. Cheng, G. T. Tietjen, J. K. Saucier-Sawyer and W. Saltzman, *Nat. Rev. Drug Discovery*, 2015, **14**, 239–247.
- 109 X. Shi, X. Yang, M. Liu, R. Wang, N. Qiu, Y. Liu, H. Yang, J. Ji and G. Zhai, *Carbohydr. Polym.*, 2021, **254**, 117459.
- 110 M. Mohammed, H. Mansell, A. Shoker, K. M. Wasan and E. K. Wasan, *Drug Dev. Ind. Pharm.*, 2019, **45**, 76–87.
- 111 C. Grune, C. Zens, A. Czapka, K. Scheuer, J. Thamm, S. Hoepfener, K. D. Jandt, O. Werz, U. Neugebauer and D. Fischer, *Int. J. Pharm.*, 2021, **599**, 120404.
- 112 W. Lin, C. Li, N. Xu, M. Watanabe, R. Xue, A. Xu, M. Araki, R. Sun, C. Liu, Y. Nasu and P. Huang, *Int. J. Nanomed.*, 2021, **16**, 2775.
- 113 C. Jin, L. Bai, H. Wu, J. Liu, G. Guo and J. Chen, *Cancer Biol. Ther.*, 2008, **7**, 911–916.
- 114 C. Jin, H. Wu, J. Liu, L. Bai and G. Guo, *J. Clin. Pharm. Ther.*, 2007, **32**, 41–47.
- 115 F. Danhier, N. Lecouturier, B. Vroman, C. Jérôme, J. Marchand-Brynaert, O. Feron and V. Préat, *J. Controlled Release*, 2009, **133**, 11–17.
- 116 C. Fonseca, S. Simoes and R. Gaspar, *J. Controlled Release*, 2002, **83**, 273–286.
- 117 Y. Dong and S.-S. Feng, *Int. J. Pharm.*, 2007, **342**, 208–214.
- 118 C. Jin, L. Bai, H. Wu, W. Song, G. Guo and K. Dou, *Pharm. Res.*, 2009, **26**, 1776–1784.
- 119 B. F. Dizaji, M. H. Azerbaijan, N. Sheisi, P. Goleij, T. Mirmajidi, F. Chogan, M. Irani and F. Sharafian, *Int. J. Biol. Macromol.*, 2020, **164**, 1461–1474.
- 120 R. Xiong, R. X. Xu, C. Huang, S. De Smedt and K. Braeckmans, *Chem. Soc. Rev.*, 2021, **50**, 5746–5776.
- 121 S. A. Hewage, J. Kewalramani and J. N. Meegoda, *Colloids Surf., A*, 2021, **609**, 125669.
- 122 J.-F. Lemineur, P. Ciocci, J.-M. Noël, H. Ge, C. Combellas and F. Kanoufi, *ACS Nano*, 2021, **15**, 2643–2653.
- 123 E. P. Favvas, G. Z. Kyzas, E. K. Efthimiadou and A. C. Mitropoulos, *Curr. Opin. Colloid Interface Sci.*, 2021, 101455.
- 124 M. Zhao, X. Yang, H. Fu, C. Chen, Y. Zhang, Z. Wu, Y. Duan and Y. Sun, *ACS Appl. Mater. Interfaces*, 2021, **13**, 32763–32779.
- 125 M. Wu, Y. Wang, Y. Wang, M. Zhang, Y. Luo, J. Tang, Z. Wang, D. Wang, L. Hao and Z. Wang, *Int. J. Nanomed.*, 2017, **12**, 5313.
- 126 D. Le Broc-Ryckewaert, R. Carpentier, E. Lipka, S. Daher, C. Vaccher, D. Betbeder and C. Furman, *Int. J. Pharm.*, 2013, **454**, 712–719.
- 127 I. M. Adjei, B. Sharma, C. Peetla and V. Labhasetwar, *J. Controlled Release*, 2016, **232**, 83–92.
- 128 K. Pušnik Črešnar, A. Aulova, D. N. Bikiaris, D. Lambropoulou, K. Kuzmič and L. J. M. Fras Zemljič, *Molecules*, 2021, **26**, 4161.
- 129 J. Chen, E. Ning, Z. Wang, Z. Jing, G. Wei, X. Wang and P. Ma, *Drug Delivery*, 2021, **28**, 1389–1396.
- 130 Y. Dong and S.-S. Feng, *Biomaterials*, 2004, **25**, 2843–2849.
- 131 Y. Dong and S.-S. Feng, *Biomaterials*, 2007, **28**, 4154–4160.
- 132 K. Wang, L. Guo, W. Xiong, L. Sun and Y. Zheng, *J. Biomater.*, 2014, **29**, 329–340.
- 133 M. Z. Ahmad, M. Rizwanullah, J. Ahmad, M. Y. Alasmay, M. H. Akhter, B. A. Abdel-Wahab, M. H. Warsi and A. Haque, *Int. J. Polym. Mater. Polym. Biomater.*, 2021, 1–22.
- 134 C. Catania, B. Muthusami, G. Spitaleri, E. del Signore and N. A. Pennell, *Clinical Lung Cancer*, 2021, DOI: 10.1016/j.clcc.2021.11.003.
- 135 J. S. Kim, S. D. Jo, G. L. Seah, I. Kim and Y. S. Nam, *J. Ind. Eng. Chem.*, 2015, **21**, 1137–1142.
- 136 Z. Todorova, O. Tumurbaatar, J. Todorova, I. Ugrinova and N. Koseva, *Eur. Polym. J.*, 2021, **142**, 110151.
- 137 R. Yang, G. Mondal, D. Wen and R. I. Mahato, *Nanomed.: Nanotechnol. Biol. Med.*, 2017, **13**, 391–401.
- 138 J. Chen, X. Fan, J. Liu, C. Gu, Y. Shi, W. Zheng and D. J. Singh, *J. Phys. Chem. Lett.*, 2021, **12**, 8170–8177.
- 139 M. C. P. Mendonça, A. Kont, M. Rodriguez Aburto, J. F. Cryan and C. M. O'Driscoll, *Mol. Pharmaceutics*, 2021, **18**, 1491–1506.
- 140 Z. Hua, T. Yu, D. Liu and Y. Xianyu, *Bioelectronics*, 2021, 113076.
- 141 X. Luan, K. Rahme, Z. Cong, L. Wang, Y. Zou, Y. He, H. Yang, J. D. Holmes, C. M. O'Driscoll and J. Guo, *Eur. J. Pharm. Biopharm.*, 2019, **137**, 56–67.
- 142 M.-Y. Hua, H.-W. Yang, C.-K. Chuang, R.-Y. Tsai, W.-J. Chen, K.-L. Chuang, Y.-H. Chang, H.-C. Chuang and S.-T. Pang, *Biomaterials*, 2010, **31**, 7355–7363.
- 143 M. S. U. Ahmed, A. Bin Salam, C. Yates, K. Willian, J. Jaynes, T. Turner and M. O. Abdalla, *Int. J. Nanomed.*, 2017, **12**, 6973.
- 144 E. J. Comparetti, G. G. Romagnoli, C. M. Gorgulho, V. de Albuquerque, Pedrosa and R. Kaneno, *Mater. Sci. Eng., C*, 2020, **116**, 111254.
- 145 Q. Guo, Y. Dong, Y. Zhang, H. Fu, C. Chen, L. Wang, X. Yang, M. Shen, J. Yu and M. Chen, *ACS Appl. Mater. Interfaces*, 2021, **13**, 13990–14003.
- 146 M. R. Bindu, P. Saranya, M. Sheeba, C. Vijilvani, T. S. Rejiniemon, A. M. Al-Mohaimed, M. R. AbdelGawwad and M. S. Elshikh, *Environ. Res.*, 2021, **201**, 111628.
- 147 Y. Wang, Y. Han, X. Tan, Y. Dai, F. Xia and X. Zhang, *J. Mater. Chem. B*, 2021, **9**, 2584–2593.
- 148 A. O. Boztas, O. Karakuzu, G. Galante, Z. Ugur, F. Kocabas, C. Z. Altuntas and A. O. Yazaydin, *Mol. Pharmaceutics*, 2013, **10**, 2676–2683.
- 149 Q. Pei, X. Hu, L. Wang, S. Liu, X. Jing and Z. Xie, *ACS Appl. Mater. Interfaces*, 2017, **9**, 26740–26748.
- 150 K. Zheng, Z. Huang, J. Huang, X. Liu, J. Ban, X. Huang, H. Luo, Z. Chen, Q. Xie and Y. Chen, *Drug Des., Dev. Ther.*, 2021, **15**, 2605.
- 151 L. A. Omtvedt, K. A. Kristiansen, W. I. Strand, F. L. Aachmann, B. L. Strand and D. S. Zaytseva-Zotova, *J. Biomed. Mater. Res., Part A*, 2021, **109**, 2625–2639.
- 152 M. Lan, L. Zhu, Y. Wang, D. Shen, K. Fang, Y. Liu, Y. Peng, B. Qiao and Y. Guo, *J. Nanobiotechnol.*, 2020, **18**, 121.



- 153 M. Eklund, F. Jäderling, A. Discacciati, M. Bergman, M. Annerstedt, M. Aly, A. Glaessgen, S. Carlsson, H. Grönberg and T. Nordström, *N. Engl. J. Med.*, 2021, **385**, 908–920.
- 154 L. Wang, B. Zhou, S. Huang, M. Qu, Q. Lin, T. Gong, Y. Huang, X. Sun, Q. He, Z. Zhang and L. Zhang, *Nano Res.*, 2019, **12**, 2451–2459.
- 155 H. Mei, S. Cai, D. Huang, H. Gao, J. Cao and B. He, *Bioact. Mater.*, 2022, **8**, 220–240.
- 156 J. Thayath, K. Pavithran, S. V. Nair and M. Koyakutty, *Nanomedicine*, 2021, **16**, 12.
- 157 N. Prajitha, S. Athira and P. V. Mohanan, *Environ. Res.*, 2019, **172**, 98–108.
- 158 A. V. Singh, P. Laux, A. Luch, C. Sudrik, S. Wiehr, A.-M. Wild, G. Santomauro, J. Bill and M. Sitti, *Toxicol. Mech. Methods*, 2019, **29**, 378–387.
- 159 W. N. Missaoui, R. D. Arnold and B. S. Cummings, *Chem.-Biol. Interact.*, 2018, **295**, 1–12.
- 160 I. Furxhi, F. Murphy, M. Mullins and C. A. Poland, *Toxicol. Lett.*, 2019, **312**, 157–166.
- 161 C. M. Keck and R. H. Müller, *Eur. J. Pharm. Biopharm.*, 2013, **84**, 445–448.

